KfK 3265
Januar 1982

The Effects of Low Doses of Different Radiation Qualities on Vicia Faba Bean Root Meristems

I. Marshall
Institut für Kernphysik

Kernforschungszentrum Karlsruhe

KERNFORSCHUNGSZENTRUM KARLSRUHE

Institut für Kernphysik

KfK 3265

THE EFFECTS OF LOW DOSES OF DIFFERENT RADIATION QUALITIES ON VICIA FABA BEAN ROOT MERISTEMS*

Ingrid Marshall

Kernforschungszentrum Karlsruhe GmbH, Karlsruhe

*von der Fakultät für Physik der Universität (TH) Karlsruhe genehmigte Dissertation

Kernforschungszentrum Karlsruhe GmbH
ISSN 0303-4003

ABSTRACT

The effects of low doses of different radiation qualities have been investigated using the micronuclei induction in Vicia faba bean roots as an indicator. The radiation qualities used were: ^{60}Co-gamma rays, high energy neutrons (maximum energy 600 MeV), low energy neutrons (mean energy 2.35 MeV), negative pions in the plateau region and negative pions in the stopping region. It was found that the best fit to the gamma ray data was obtained by using a linear+quadratic relationship, $E=C+\alpha D+\beta D^2$, while in the case of the other radiation qualities a linear equation, $E=C+\alpha D$, represented the best fit, implying the non-existence of a threshold dose. No dose-rate, fractionation or oxygen effect was found for gamma radiation in the low dose region (below 20cGy) where the linear dependence between effect and dose is dominant. In contrast, in the high dose region these effects were present as normally expected. Fractionation experiments were carried out using high energy neutrons and pion radiation. No recovery was observed after neutron radiation while some recovery was found for the pion radiation. The RBE values found for the two neutron energies were in the high dose region 4.7±0.4 (600 MeV neutrons) and 11.8±1.3 (2.35 MeV neutrons). In the low dose region the RBE value approached a constant value of 25.4±4.4 for the high energy neutrons and 63.7±12.0 for the low energy neutrons.

DIE WIRKUNGEN KLEINER DOSEN VERSCHIEDENER STRAHLENQUALITÄTEN AUF DIE WURZELMERISTEME DER BOHNE VICIA FABA.

Die Wirkungen kleiner Dosen verschiedener Strahlenqualitäten auf die Bohne Vicia faba wurden mittels der Mikrokern-Bildung untersucht. Die verwendeten Strahlenarten waren: ^{60}Co-Gamma-Strahlen, hochenergetische Neutronen (maximale Energie 600 MeV), niederenergetische Neutronen (mittlere Energie 2.35 MeV) und negative Pionen in dem Plateau und Bragg-Peak Bereich.

Die linear und quadratische Verbindung : $E = C + \alpha D + \beta D^2$ ergab die beste Anpassung an die Gamma-Daten, während sich die anderen Strahlenarten besser durch eine lineare Gleichung $E = C + \alpha D$ darstellen ließen. Diese Linearität impliziert, daß es keine Schwellendosis gibt.

In der niedrigen Dosisregion (unter 20cGy), in der eine lineare Abhängigkeit zwischen Dosis und Wirkung dominiert, konnte kein Dosisraten-, Fraktionierungs- und Sauerstoffeffekt festgestellt werden. Im Gegensatz hierzu wurden in der hohen Dosisregion die normalerweise erwarteten Effekte gefunden.

Fraktionierungsexperimente wurden auch mit hochenergetischen Neutronen und negativen Pionen ausgeführt. Nach der Neutronenbestrahlung ließ sich keinerlei Erholung feststellen, während im Falle der Pionenbestrahlung etwas Erholung beobachtet wurde.

Die RBW-Werte für die zwei Neutronenenergien lagen im hohen Dosisbereich bei 4.7 ± 0.4 (600 MeV Neutronen) und 11.8 ± 1.3 (2.35 MeV Neutronen). Im niederen Dosisbereich erreichte der RBW-Wert einen konstanten Wert von 25.4 ± 4.4 für die hochenergetischen Neutronen und im Falle der niederenergetischen Neutronen einen Wert von 63.7 ± 12.0 .

CONTENTS

	Page
CHAPTER I. INTRODUCTION	1
CHAPTER II. SHAPE OF THE DOSE EFFECT CURVE	4
CHAPTER III. BIOLOGICAL SYSTEM	10
1. Morphology of the bean Vicia faba	12
2. Tests performed with the Vicia faba system	14
2.1 Ten-day growth	15
2.2 Mitotic index	16
2.3 Micronuclei	16
3. Conditions modifying radiation response	20
3.1 Dose fractionation	20
3.2 The dose rate effect	21
3.3 The oxygen effect	21
CHAPTER IV. MATERIALS AND METHODS	23
1. Culture system	23
2. Irradiation containers	25
3. Hypoxic irradiations	28
4. Preparation of the biological material	28
5. Mathematical analysis of the experimental data	29
CHAPTER V. DOSIMETRY	32
1. Interactions of γ-rays with tissue and their dosimetry	33
2. Interactions of neutrons with tissue and their dosimetry	35
2.1 SC-neutron beam dosimetry	36
2.2 ^{252}Cf-neutron dosimetry	40
3. Interactions of pions with tissue and their dosimetry	42

Page

CHAPTER VI. RESULTS 46

1. Single dose exposures 48
   1.1 SC-neutron results 48
   1.2 ^{252}Cf-neutron results 54
   1.3 ^{60}Co-gamma results 54
   1.4 π^- plateau and π^- peak 62
2. Split dose experiments 64
   2.1 SC-neutrons 65
   2.2 ^{60}Co-γ rays 65
   2.3 π^- plateau and π^- peak 66
3. Oxygen effect 67
4. RBE values 70

CHAPTER VII. DISCUSSION 73

SUMMARY 83

CHAPTER I

INTRODUCTION

The recent developments of nuclear technology, like nuclear power plants and nuclear weapons, and also the increasing use of ionising radiation in medicine, have brought the problems of possible health effects produced by low doses of radiation into the center of public interest. One of the main questions still discussed is as to whether or not a so called threshold dose exists, i.e.the dose below which no radiation damage is produced. This threshold dose should, however, not be confused with the threshold dose observed in toxicology where an organism can survive up to a certain critical dose but will die if the dose is exceeded. In the case of ionising radiation it has been shown that in the high dose region an increase in radiation dose will also result in an increase in effect. How far this relationship extends into the low dose region is still widely discussed.

The recently published BEIR III - report on the Biological Effects of Ionizing Radiation [1], where most of the relevant data collected up to now on the effects of radiation are reported, was not able to answer this question. The problems of measuring small radiation effects stems from the fact that the sample size required to estimate or to test a small absolute effect such as cancer induction after low doses of radiation is extremely large. In 1980 data from a health survey made in China were published [2]. Researchers studied the health status of about 73,000 people living in regions where the

radiation level is three times that found in the neighboring areas. There were 77,000 inhabitants in the control regions. No increase in malignancy in the high background area was observed. Could those results mean that there really exists a threshold dose, or could it actually mean that the sample size has still been too small and it was therefore not possible to ascertain the effect statistically? Even if a population size of two times 70,000 seems large the following might clarify the problem. The sample required to estimate or test an excess is approximately inversely proportional to the square of the excess. For example, if the excess is linearly proportional to dose and if 1000 exposed and 1000 control persons are required to test the cancer excess adequately at 100 cGy[1], then about 100,000 people in each group are required at 10 cGy, and about 10,000,000 in each group are required at 1 cGy [3]. This demonstrates how difficult it is to find the proper dose response curve for an organism if only "gross" effects are studied. However, it is known that the damage finally observed after irradiation of an organism has first been produced on the cellular level. It seems therefore reasonable to study the effect of radiation directly on the cellular basis and thus, because of the large numbers automatically involved, improve at the same time the statistical significance of the result.

In order to contribute to a better understanding of the shape of the dose-response curve at low dose levels, we have performed experiments with different kinds of ionizing radiation using the broad bean Vicia faba as a biological test system.

As regards the general validity of the results, there seems to be no disadvantage in using a plant system as opposed to an animal system since both are eucariotic systems (organisms whose chromatin is contained in a nucleus) and their chromosomes are similar in struc-

---

[1] 1 cGy = 1 rad = 10^{-2} J/kg

ture and in the basic biochemistry. The mechanisms by which ionizing radiation induces mutations or chromosome aberrations in plants are similar, if not identical, to those in mammals. In addition, very large populations of plants or plant cells can be grown and analyzed relatively easily.

The decision for selecting this particular system is based on the following requirements :

i) The system should represent an organism.

ii) It should have a sufficiently high intrinsic sensitivity to radiation, enabling measurements at low doses to be performed.

iii) More then one effect should be testable.

iv) The system should be well established and easy to handle.

It will be shown in the following sections that Vicia faba has all these properties.

The next two chapters, "the shape of the dose effect curve" and the "biological system" should actually be regarded as a continuation of the introduction. There the physical and biological meaning of the dose effect curve and the advantages of using Vicia faba will be discussed in more detail. Chapter IV. is dedicated to the material and methods section and chapter V. to the dosimetry. The presentation of the results found for the different radiation qualities and the different test systems used is discussed in chapter VI. and will be concluded with a discussion of the implications of these findings.

CHAPTER II

SHAPE OF THE DOSE EFFECT CURVE

The irradiation of biological material results in the production of a certain amount of damage which depends on the dose administered. This relationship between radiation dose and effect is described by the dose effect curve. Since the damage produced will normally reduce the surviving capacity of the system, the dose effect curve is related to the survival curve. Therefore there are two equivalent procedures to describe radiation damage: (a) Effect curve : Number of events, eg. chromosome aberrations per cell. (b) Survival curve : Fraction of surviving cells (see also Table 1). In figure (1) an example of a survival curve is shown.

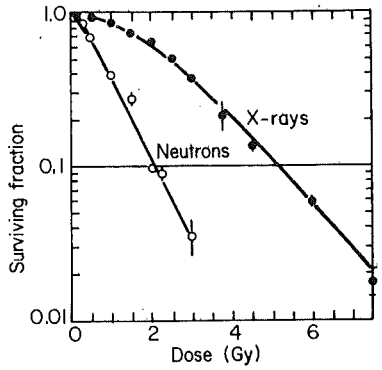

Figure 1: Example of a survival curve after neutron and X-ray irradiation (redrawn from [4])

Many theories have been developed in order to give a qualitative and quantitative description of the shape of the survival curve. From the classical investigations of Dessauer [5], Blau et al.[6], Lea [7], Timofeeff-Ressovsky and Zimmer [8] the "Target Theory" was

developed. This theory uses the fact that radiation is delivered to the biological material in discrete energy packets which are statistically independent and follow a Poisson distribution. The main objection against the target theory is that it does not adequately account for repair processes within the biological target that are known to influence its response. Repair is the basis of another theory which has been recently developed, namely the repair- misrepair model by Tobias et al.[9].

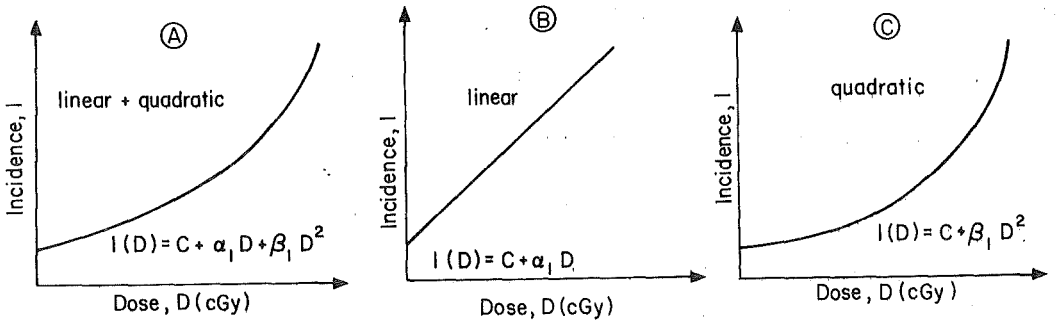

Figure 2: Three possible shapes of a survival curve

A dose effect relationship commonly used today is the linear-quadratic dose dependence of radiation induced effects. In figure (2) three examples of the possible shapes resulting from such a model are given. Figure (2a) represents a curve where both the linear and the quadratic term play an important role. Figure (2b) is an example of a purely linear relationship between incidence and dose, while in figure (2c) only the quadratic term contributes to the incidence. This type of relationship was suggested by Lea in 1946 [7] and was also used by Leenhouts and Chadwick [10] to describe their molecular theory, but mainly since the development of the theory of dual radiation action has it gained a physical basis. As the concept of this theory is quite fundamental for comparing different types of ionizing radiations, it will be outlined briefly.

The theory of dual radiation action published in 1972 by Kellerer and Rossi [11] is based on microdosimetric principles. What is nor-

Table 1: Different effect- and survival-curves.

Relationship	Radiation-induced Effect	Survival
Linear	$E = \alpha D$	$N/N_0 = \exp-(\alpha' D)$
Quadratic	$E = \beta D^2$	$N/N_0 = \exp-(\beta' D^2)$
Mixed	$E = \alpha D + \beta D^2$	$N/N_0 = \exp-(\alpha' D + \beta' D^2)$

mally measured as dose D is the integral dose over a macroscopic volume. But radiation does not deposit its energy in a uniform way at the microscopic level. It is therefore necessary to consider a microdosimetric quantity, the specific energy z. Like the absorbed dose D, the specific energy is defined as energy divided by mass, but denotes values of this quotient in a localized region (eg. the cell nucleus). The variations of z are described by the probability distribution f(z,D), a composite Poisson distribution which depends on the shape and size of the reference volume and on the radiation quality. If a very small volume or a densely ionizing particle is considered then the fluctuations are greatest, while for large volumes and large doses of sparsely ionizing radiations z is near in value to D. The importance of this quantity becomes apparent if one determines the values of z in cell nuclei that have received about 1 year of background radiation. This produces an absorbed dose of about 1 mGy of mostly low-LET[1] radiation. In about two-thirds of the nuclei z=0, that is, no ionizations have occured; in the remainder, z varies over several orders of magnitude, with an average value of about 3 mGy. If the same dose, D, was delivered by fission neutrons, z would differ from zero in only 0.2% of the cell nuclei; however, in these affected nuclei it would average 0.5 Gy, i.e., 500 times the average dose. Likewise, a 1 MeV electron passing through the nucleus of a

[1] LET stands for Linear Energy Transfer and is also known as dE/dx (Bethe Bloch formula).

cell produces only a few dozen ionizations in the nucleus. For the much slower heavy particles, such as protons or α-particles, the ionisation density is higher. Thus, a 1 MeV proton produces several thousand ionisations when it traverses a cell nucleus. Therefore, one single heavy particle traversing the cell nucleus has a considerable probability of killing a cell or causing mutations. In contrast, several thousand of the electrons liberated by X- or γ- rays must traverse a cell before it is likely to lose its proliferative capacity [12]. Figure 3 shows an example of the different ionization densities found for several particles and kinetic energies. The background of the figure represents a cell nucleus with a mitochondrium inside. For the 500 KeV proton it was not possible to indicate all ionizations in one line; therefore a widening of the track was made [13]. It is evident that the heterogenity of energy deposition depends greatly on radiation type.

In cells which have been affected by radiation, elementary lesions can be produced (eg.DNA strand break), the number being proportional to the microdose within the sensitive site. It is commonly assumed that the loss of proliferative capacity of cells, and also their transformation which may lead to carcinogenesis, are linked to chromosomal aberrations. These aberrations are caused by pairs of lesions, eg. by two neighboring chromosome breaks, which might be, if they were produced close enough to each other in space and time, incorrectly joined together during of the repair process. A description of a possible mechanism for the production of chromosome damage will be given in chapter III. section 2.3. In the case of sparsely ionizing or low-LET radiation each of the interacting sublesions will usually be produced by independent ionizing particles. In this case the number of biological lesions will be proportional to the square of the radiation dose.In the case of high-LET radiation where the

Figure 3: The ionization densities of different particles.

lesion can be produced by only one particle the biological effect will be directly proportional to dose. Therefore the yield of elementary lesions ϵ can be expressed by the following equation:

$$\epsilon = k(\xi D + D^2)$$

The variable, ξ, determines the linear component of the dose effect relationship and is therefore an important parameter of radiation quality. It has such small values for X- rays that at high doses the linear term can be discounted, while in the case of neutrons it has such a large value that the quadratic term in D can usually be neglected.

CHAPTER III

BIOLOGICAL SYSTEM

Root meristems have been extensively used in cytological and radiobiological research because of their ease of handling and the general applicability of the results to broad general problems in radiation biology. Already as far back as in 1913 Mottram [14] used this plant to study the effects of ß-radiation. Howard and Pelc [15] first elucidated the cell cycle components(G1,S,G2) of interphase in Vicia faba. Thoday and Read [16] discovered with Vicia faba that chromosome aberrations are produced at a reduced rate when oxygen is absent during radiation. In his now "classical" work on the repair of radiation induced chromosome damage Sax [17] utilized also root meristems. Soon after the discovery of the neutron in 1932 experiments were made using Vicia faba to study the difference in effect between gamma rays and neutrons by Gray,Read and Mottram [18]. In 1951 Gray and Scholes [19] published a series of papers on the morphology and the cell kinetics of Vicia faba. A review of all the important papers written up to 1959 on bean roots was published by Read [20]. In comparing the results obtained for broad beans and those found in mammalian systems, he concluded that the effects exhibited were rather similar. Also during the past 10 years Vicia faba has been used by the Radiobiology Group at CERN [21,22,23] as one of the test systems to study radiation effects. As a result of this long term and thorough investigation, the bean root is a relatively

well understood system. However, as with other systems, there are advantages and disadvantages for its use as test material.

Advantages:

The material is easily available throughout the year. It is inexpensive and easy to grow and handle. The method does not require sterile conditions or any expensive material or equipment.

The root meristem contains a high proportion of cells in mitosis (≈10%), which is of advantage when chromosome aberrations are to be analyzed.

The chromosome number is low (2n=12) and the chromosomes very large, which makes the analysis of chromosome aberrations easy and accurate. An idea of the size of the Vicia faba chromosomes may be obtained by comparing the DNA content and chromosome number of a Vicia faba cell with those of Chinese hamster or human cells, two other materials commonly used for studying the production of chromosomal aberrations. A root tip cell of Vicia contains about 46 pg of DNA which is distributed among 12 chromosomes, a Chinese hamster cell 8.3 pg of DNA distributed among 22 chromosomes, and a human cell 7.3 pg of DNA distributed among 46 chromosomes [24].

Finally, in contrast with in-vitro systems such as cultured animal and plant cells, root-tip cells have a very low spontaneous aberration frequency and a stable chromosome number.

Disadvantages:

The cell wall constitutes an obstacle to both biochemical and cytological studies on plant root tips. The pectic substance in the middle lamella of the cell wall has to be dissolved by hydrolysis with acids or enzymes before squash preparations can be made and good separation of the cells can be obtained.

It is also nearly impossible to obtain more than a very moderate synchrony of the cell division .

Finally, I should mention still another disadvantage which in an other way could be looked upon as an advantage. Although the root tip contains a variety of cell types having different mitotic cycles and perhaps different sensitivities to treatment, the symbiotic effect of these cells should give a more realistic picture of what is actually happening in an organism after irradiation.

1. Morphology of the bean Vicia faba

A photo of the bean is shown in figure (4). The shoot and the lateral roots have been removed leaving only the cotyledon and the main root. The roots are normally irradiated in this condition. In figure (5) the interior of the main root tip is shown. The first 1/3 mm consists of the root cap, which contains relatively inert cells. The meristem itself where the cells are actively dividing, occupies the next 3 mm of the root. Inside the meristematic region, which contains about $2.6*10^5$ cells [19,20], is a small part, the quiescent center, containing about 500 cells which rarely divide, if at all [25]. This is followed by the elongating zone. Here the cells do not divide anymore but differentiate and elongate. This elongation of cells causes the increase in length of the root. The rest of the root tip consists of mature cells which are fully elongated.

It was shown by Gray and Scholes [19] that the mitotic index (see also section 2.2) follows an approximate Gaussian spatial distribution only in the first 1.5 mm of the meristematic region (fig.6). Thereafter, the number of actively dividing cells drops rapidly the closer the cells are to the elongating zone. They observed that within the region of 1.5 mm the intermitotic cycle time (the time between cell division) has an average value of about 19 hours, while the division itself takes place in about 2.6 hours. In general cell cycle times between 19 and 30 hours have been found for Vicia faba

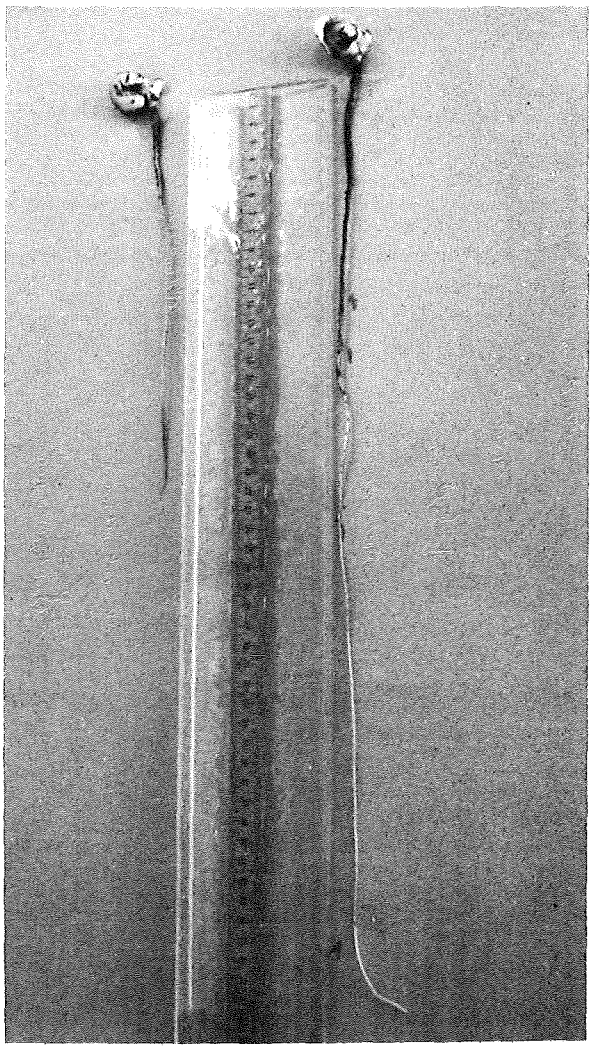

Figure 4: The bean Vicia faba: non irradiated and irradiated.

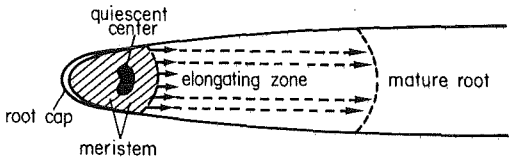

Figure 5: The interior of the main root tip.

[15,19,26]. We have assumed a cycle time of 24 hours, which seems to agree with the experimental data very well.

Only the meristematic region of the root is of interest for this investigation, because it is here that cells are actively dividing

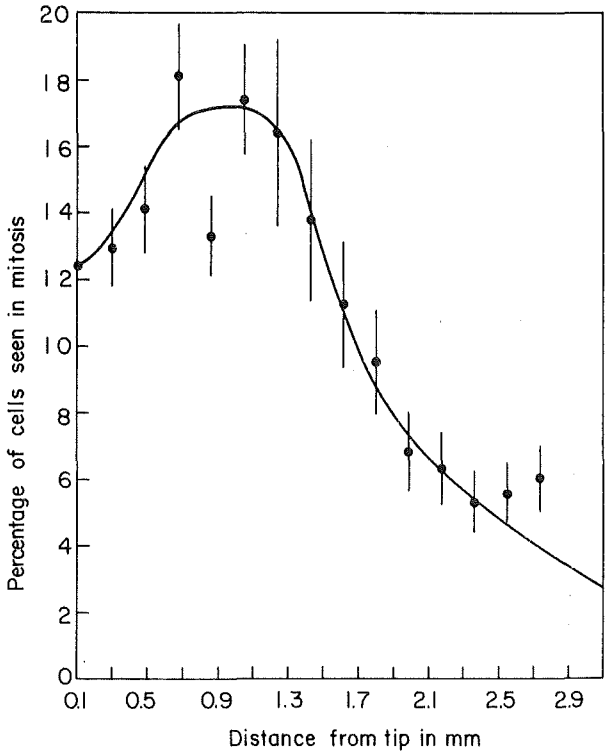

Figure 6: The mitotic index distribution as a function of distance from the root tip.

and where radiation produces the damage which reduces the surviving capacity of the bean root. Gray and Scholes [19] were able to demonstrate this with a simple experiment. In one case they irradiated the whole bean, while with an other group of beans they shielded the upper part and irradiated only the meristem; with a third group they irradiated only the upper part and shielded the meristem. Only when the whole bean or the meristem itself was irradiated was a reduction in growth observed.

2. Tests performed with the Vicia faba system

The first test, the 10 day growth, was used only as a monitor of the overall response of the complete organism. The micronucleus test together with the analysis of the mitotic index were actually the ones of main interest. With those the effect of dose rate, dose fractionation and oxygen on the bean root in the low dose region was investigated.

2.1 Ten-day growth

For the determination of the 10 day growth the length of the root is measured daily after irradiation. In this way both the daily growth increment and the total growth increment 10 days after irradiation can be determined. Dividing the 10 day growth by the corresponding value of the non irradiated control group results in the percentage 10 day growth. Plotting these values over dose results in a curve (fig.7) which is rather similar to a survival curve. This fact is not very suprising because the reduction in growth has been produced through cell killing. Many 10 day growth curves have been established in the last 10 years in the radiobiology group at CERN for a large number of radiation qualities, dose-rates and different dose modifying factors [22, 23]. The results found, have shown the good reproducibility of the system, as well as its comparability with animal and human results.

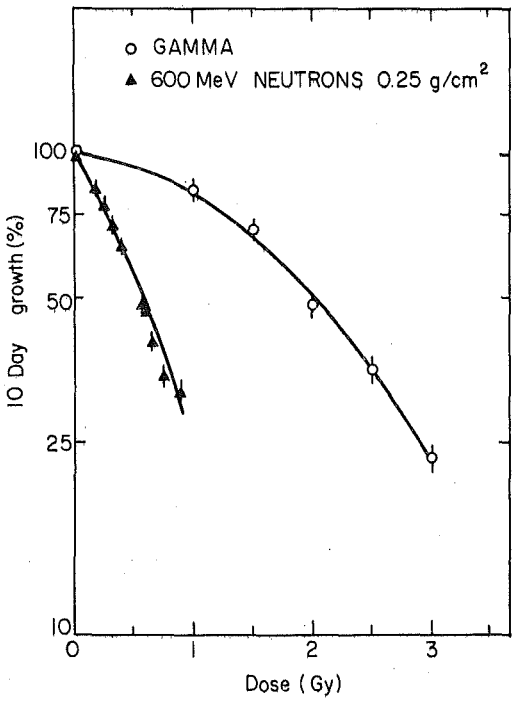

Figure 7: The percentage 10-day growth relative to the control group as a function of dose: after gamma irradiation and after neutron irradiation[23].

2.2 Mitotic index

The mitotic index gives the fraction of cells in mitosis (prophase, metaphase, anaphase, telophase). It is only in this period of the cell cycle that the chromosomes are visible, while during the remaining 90% of the cycle the chromatin in the nucleus has a diffuse appearance. The mitotic index is not only of interest as a test by itself but it is also important in combination with micronuclei induction. In fact cells have first to go through mitosis before a micronucleus is formed and, therefore, any change in the mitotic index should be reflected in a change in the number of micronuclei produced. This fact will be discussed more thoroughly in the result section.

2.3 Micronuclei

A striking abnormality that can be observed after radiation in actively proliferating tissues is the appearance of more than one nucleus in a cell. These additional nuclei, which have been termed micronuclei because they are relatively small in comparison to the main nucleus, arise from acentric fragments which can be induced by radiation or by a chemical agent. In figure (8) a simplified description is given of how an acentric fragment can be produced by radiation. The moment radiation has broken two adjacent chromosomes or chromatids four possible reactions can occur. In case A) complete repair has taken place. In case B) no attempt to repair the damage was made at all. In case C) the broken ends exchange symmetrically and in case D) asymmetrically.

Figure 9 shows what will happen during mitosis after those repair-misrepair attempts have taken place. In case A) real repair has taken place (see also figure (10) for an example of a normal anaphase). In case B) 2 fragments are unattached during anaphase

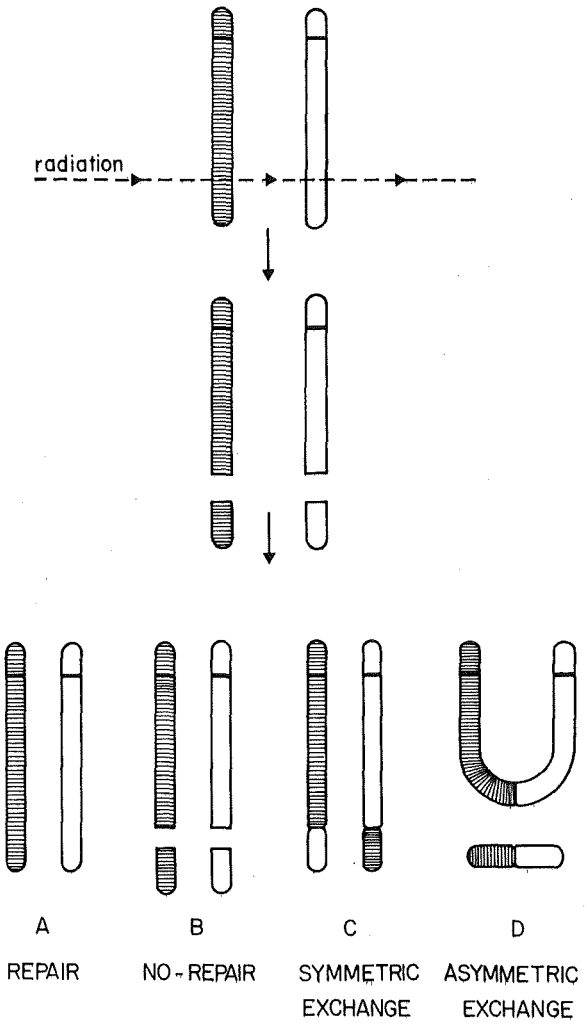

Figure 8: A shematic description for the production of chromosome aberrations after irradiation.

because the centromere which normally pulls the chromosomes to the opposite poles is missing (acentric).

An example of an anaphase with fragments is given in figure (11).

The aberration in case C) is only visible with special staining techniques. Finally in case D) the chromosome aberration produced by the misrepair has resulted in a dicentric (2 centromeres) and an acentric fragment. The chromosome with the two centromeres might be pulled to opposite poles during anaphase and form a so called anaphase bridge. In figure (12) an example for such a bridge is given.

There are two possibilities concerning the fate of this anaphase bridge. One is that the bridge will finally rupture (fig.13) and the

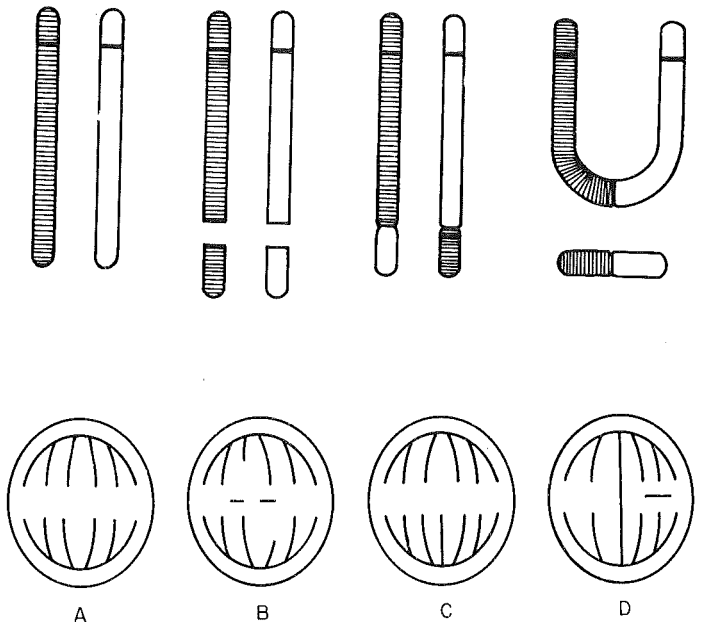

Figure 9: The fate of the chromosome aberrations shown in figure 8 during mitosis.

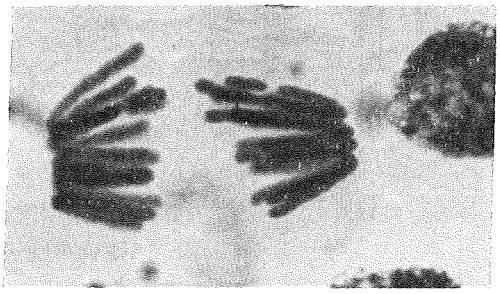

Figure 10: An example for a normal anaphase.

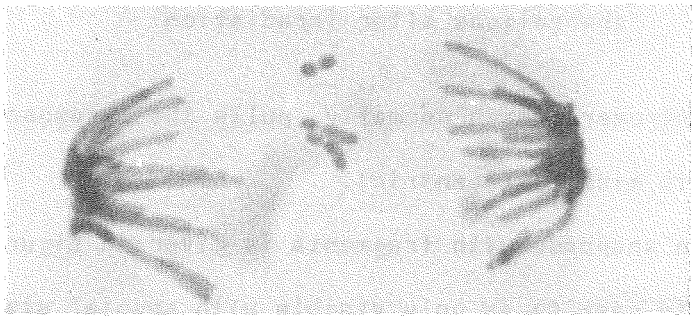

Figure 11: Anaphase with fragments.

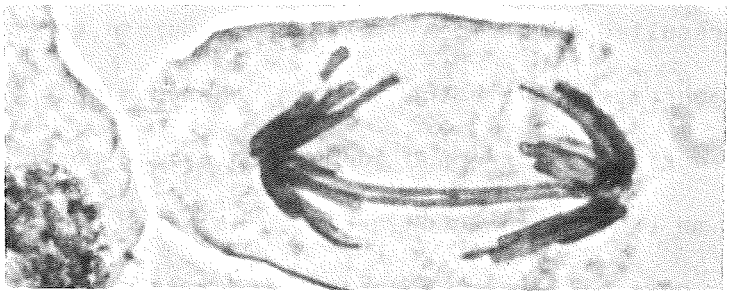

Figure 12: An example for an anaphase bridge.

other that one chromosome end will pull the other one to the opposite site (fig.14).

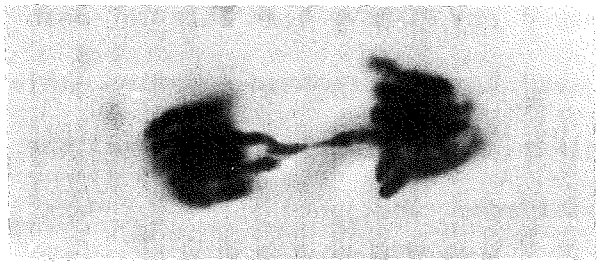

Figure 13: An anaphase bridge which is going to rupture in the middle.

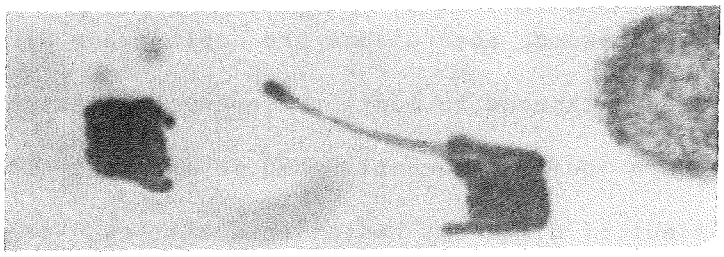

Figure 14: A chromosome is pulled to the opposite site.

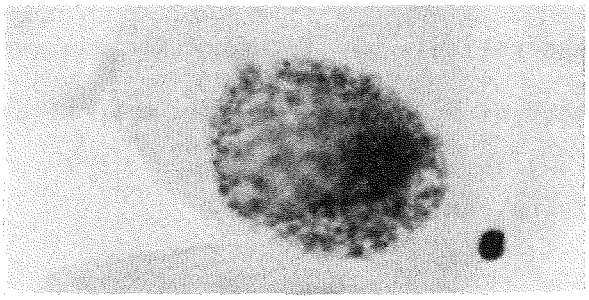

Figure 15: A cell containing a micronucleus.

Those acentric fragments then form micronuclei in the interphase following mitosis and can be observed in one or both daughter cells (fig.15). Micronuclei which are produced as a result of radiation damage can therefore only be seen in cells which have undergone division since the irradiation. The capability of acentric fragments to form micronuclei indicates that they can still perform at least those condensation functions related to mitosis and also the subsequent chromosomal despiralization and nuclear envelopment processes necessary for the formation of a nucleus. This can be easily seen from the

fact that because Vicia faba represents an asynchronous cell population, cells have been irradiated in all stages of the cell cycle . Cells which were damaged in G1 have been able to pass through the S and G2-phase before they finally reached mitosis. This implies that chromosome fragments are at least able to survive one complete cell cycle and have at least some functional ability. Because micronuclei are formed from chromosome aberrations and chromosome aberrations can be produced by radiation or chemical agents, there must also be a correlation between micronuclei induction and radiation or chemical dosage. Since chromosome aberrations are relatively difficult to score, it can be advantageous to monitor micronuclei instead. Indeed this effect has been quite frequently used in the past to study the difference in effect of different radiation qualities, or the effect of oxygen [27]. Recently the micronucleus test in general has been proposed independently by Schmid [28,29] and Heddle [30] as a much more rapid, easy and reliable way to score for mutagens, other than the traditional method of scoring chromosome aberrations.

3. Conditions modifying radiation response

3.1 Dose fractionation

If a dose of low LET radiation is not delivered all at once but divided into two equal fractions with enough time between the irradiations for recovery to take place, less damage and therefore a higher survival rate is found. Elkind [31] has shown that this effect can be ascribed to the independent action of each radiation dose. The following figure (16) which is redrawn from this reference is a good example for this. If a dose of 5 Gy (relative survival=0.1) is repeated after 18 hours the survival is again about 0.1 of the the previous 0.1 resulting in a final survival of close to 0.01. This fact is commonly referred to as repeating the shoulder of the survi-

val curve. Because the capacity of recovery from radiation damage seems to be related to the size of the shoulder of the survival curve, the smaller the shoulder the less recovery should be expected. In the case of linearity no difference between effects from fractionated doses and single doses should be found. This lack or only small amount of recovery in the case of high LET radiation has been recently reported by several groups [32,33,34,35,36,37].

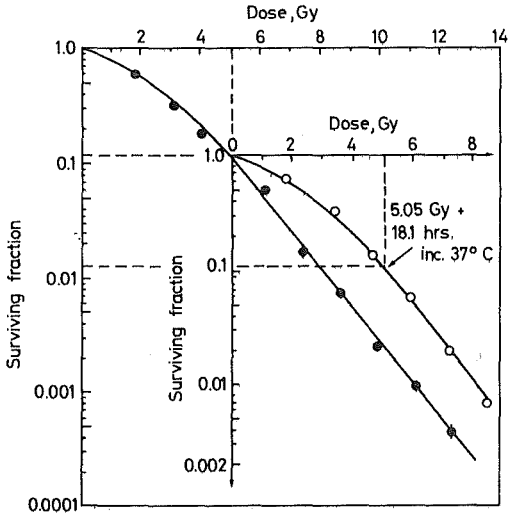

Figure 16: An example of the fractionation effect

3.2 The dose rate effect

In the case of low LET radiation a considerable difference in effect is observed if the same radiation dose is delivered at a high or at a low dose rate [7,20]. Administering the dose at a low dose-rate is equal to an ultra fractionation scheme with the number of fractions approaching infinity. This results in a continous repetition of the shoulder thus modelling a flattening of the survival curve (see fig.17).

3.3 The oxygen effect

It is a known fact that if the amount of free oxygen normally present in a biological system is reduced drastically and irradiations are carried out, then less effect will be observed. This fact is com-

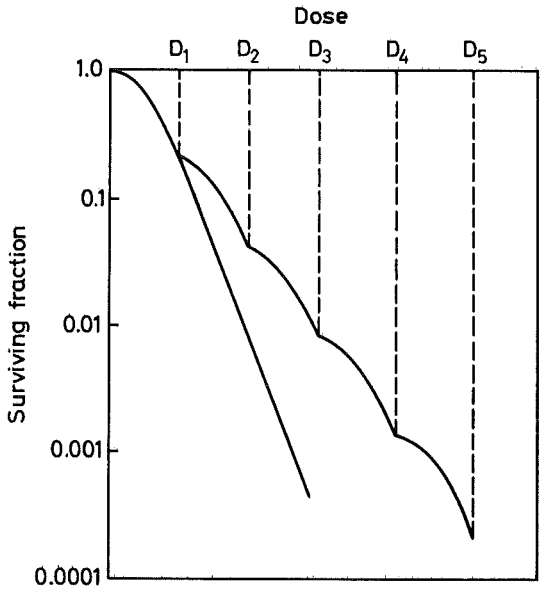

Figure 17: An example of the dose-rate effect.

monly referred to as the oxygen effect. The mechanism of this oxygen effect is not yet fully understood. What is generally agreed upon is that oxygen acts at the level of free radicals (R) produced by radiation. This reaction results in RO_2, an organic peroxide which changes the chemical composition of the material. These chemical changes initiate a chain of events resulting in the final expression of biological damage. If no oxygen is present this reaction cannot take place and the ionized molecules can recover the ability to function normally. It is therefore said, that the oxygen fixes lesions produced by radiation [38].

However, there is also only a small oxygen effect observed in the case of high LET radiation. If in the case of low LET radiation the oxygen enhancement ratio (OER) is found to be between 2 and 4, it lies between 1 and 2 for high LET radiation [39,40,41,42,43,44,45]. This OER value is the ratio of the doses needed to produce the same effect if oxygen is absent or present in the irradiated material.

CHAPTER IV

MATERIALS AND METHODS

1. Culture system

The method of culture of the broad bean is in general the same as has been described by E.J.Hall in 1961 [44]. About 3 times the number of beans finally needed for the experiment were soaked in culture tanks containing fresh, aerated, filtered tap water.The water flow rate through the tanks was about 2 liters per minute and the water temperature was thermostatically controlled to stay at 19.0 ± 0.1 ^{0}C (fig.18). After 3 days, when the root tip started to break through the skin, the beans were planted in moist, sterilised vermiculite, a medium used to raise seedlings. The containers were covered to prevent the vermiculite from drying out. After a growing period of 3 days the beans were taken out of the vermiculite and the testa and the plumule were removed. Beans that were damaged eg. exhibiting a double meristem or attacked by fungi or were shorter than 30 mm were eliminated. A minimum length of 30mm was necessary for the root to reach the water in the growing tank.

A number was written with ink on the cotyledon of each bean and the length of the root from the cotyledon down to the root tip was measured and recorded. Then the beans were transferred to the growing tank where they were placed on a perforated PVC support, allowing the roots to be in contact with the water while the cotyledons stayed

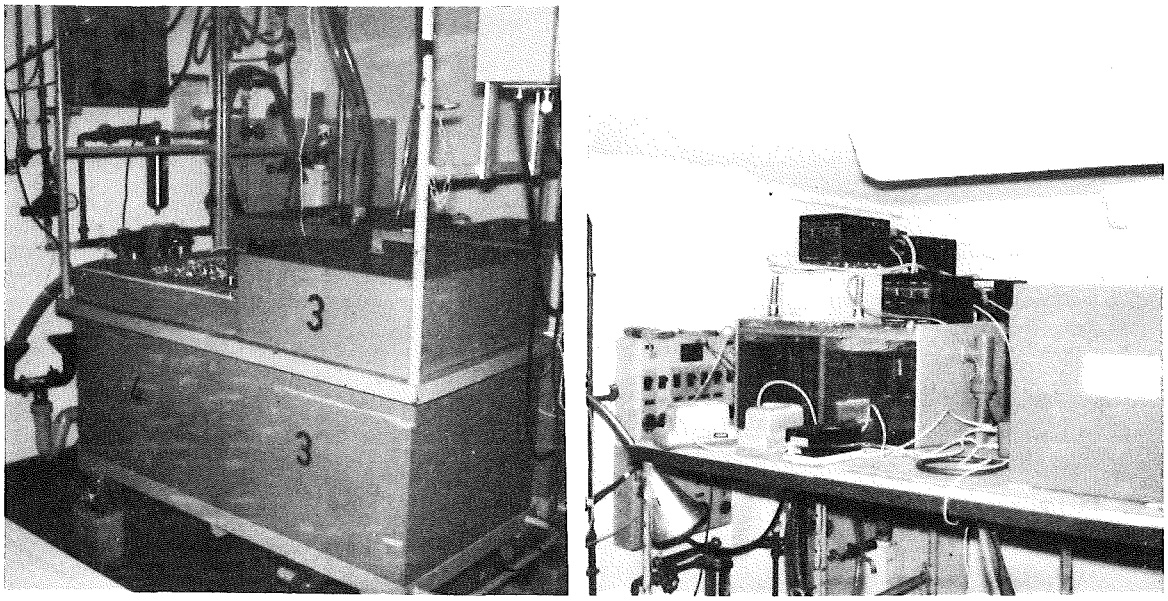

Figure 18: The culture tank and the temperature control unit.

dry in air (fig.19).

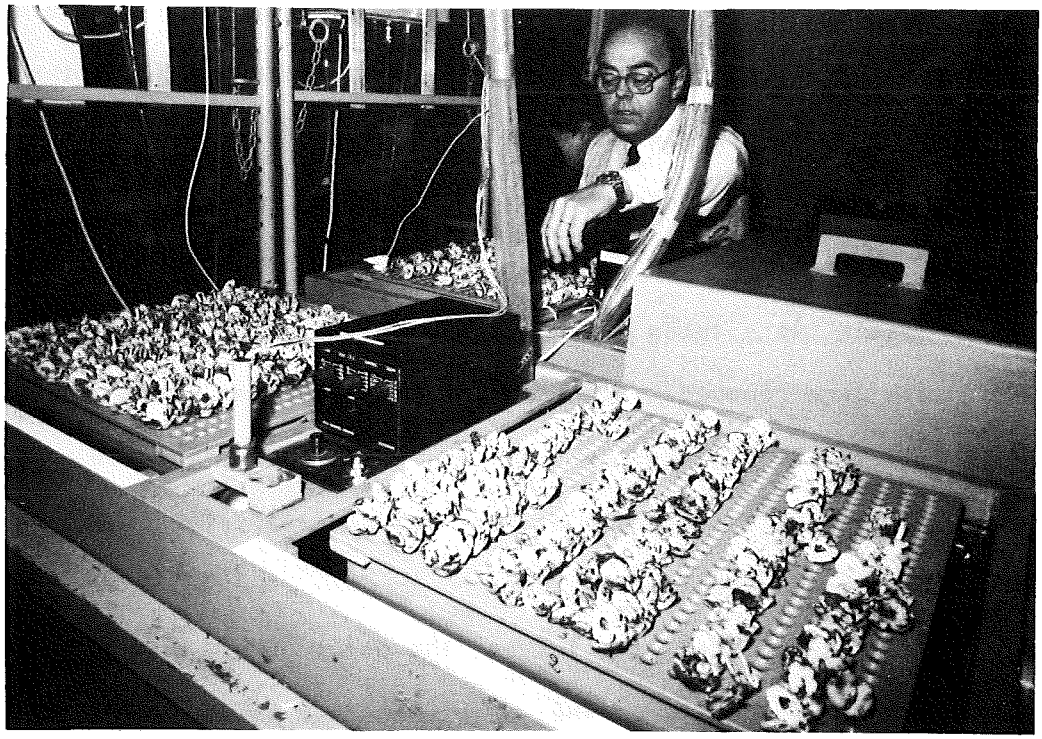

Figure 19: Beans growing in culture tank.

Three days later each bean was remeasured, its new length recorded

and the length increment calculated. The beans were now selected according to their length and growth. Only beans with a length and growth rate within one standard deviation of the mean value were used for the experiment.The following day the beans were sorted into groups and put into special irradiation containers. The number of beans in a group varied between 25 and 40 depending on the experimental test chosen, eg. 10 day growth or micronuclei induction . The irradiation containers were connected to a system comprising a refrigerated water bath, a thermostatically controlled heater and an air pump, and was commonly referred to as the "cooler" (fig.20). The water temperature was kept constant at 19.0 ± 0.1 °C by adjusting the refrigerator and the heater.

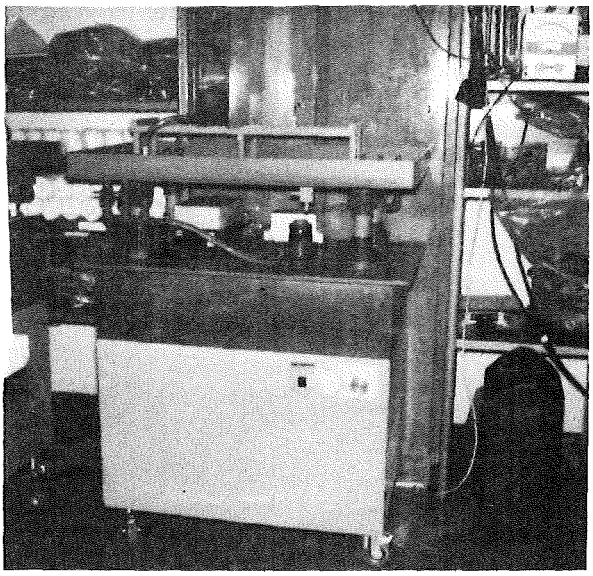

Figure 20: The cooler.

2. Irradiation containers

Three types of radiation containers were employed. The rectangular container was used for gamma and high energy neutron irradiation, where the beam was extracted horizontally. The round radiation container was used for the pion irradiation where the beam was extracted

vertically.The cylindrical shaped container was used for the experiment with ^{252}Cf - neutrons.

In the box shaped container, the bean holder could be placed in two different positions (fig.21). In the front position the beans are kept very close to the "window" of the PVC container. The "window" stands for a circular region where the thickness of the container is reduced to 1 mm. The final absorber thickness in front of the root tip, including the water surrounding the beans, is then about 3 ± 1 mm. This position is normally chosen for neutron experiments, while for the gamma radiation the middle position is used (22). Because of the difference in beam size, depending on what radiation is used, a circular ink mark is made on the net which holds the beans in place, corresponding to the size of the beam and defining in this way the maximum permissible area of the meristem location.

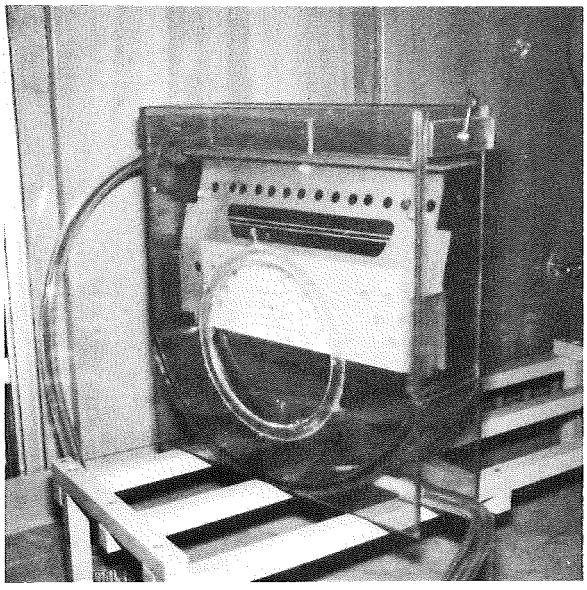

Figure 21: Box-shaped irradiation container.

The container used for the pion experiment is shown in figure (23).

All the roots have to be positioned in such a way that their meristems are confined within the circular region in the middle of the

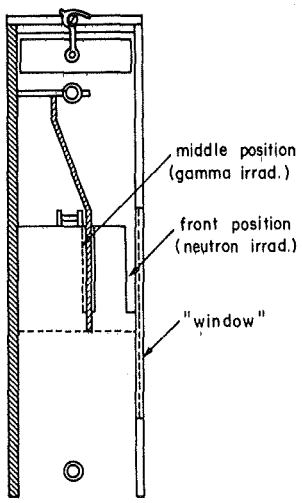

Figure 22: Side view of the box shaped irradiation container.

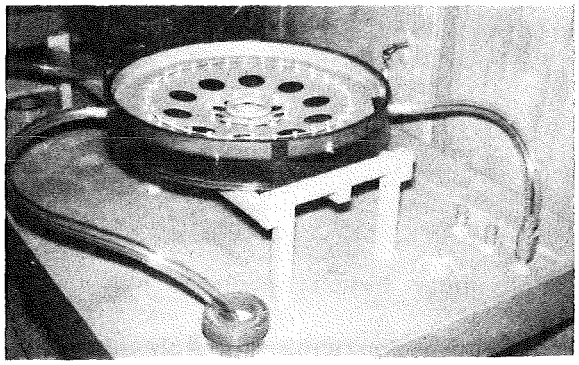

Figure 23: The container used for the pion irradiations.

container, where the beam is passing through. The third container (fig.24) was used for the low energy neutron experiment. It was constructed in such a way that the source could be positioned in the middle of the cylindrical shaped container. The beans were held in place alongside the inner plastic wall with the help of a net on which the radiation area was marked.

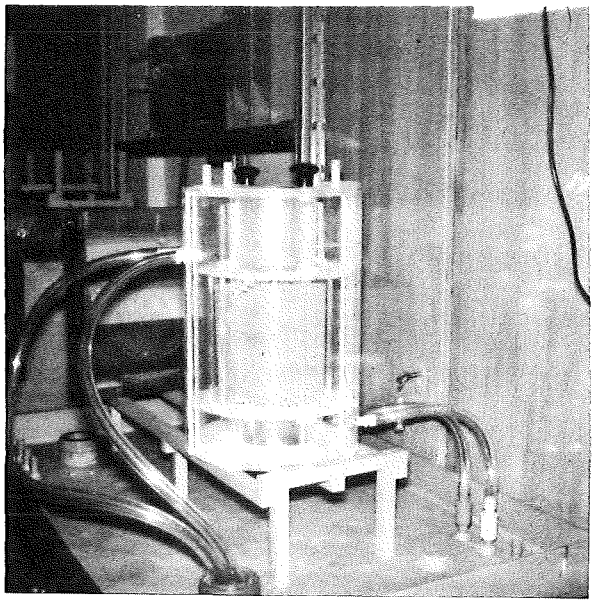

Figure 24: The container used for the low energy neutron irradiation (^{252}Cf-neutrons).

3. Hypoxic irradiations

For the irradiation under hypoxic conditions the beans were transferred to their irradiation containers which were then closed with an air tight lid and connected to the cooler. There was a continous flow of nitrogen into the water of the cooler system and therefore also through the water in the irradiation tank. Furthermore, the air gap between the cotyledon of the beans and the lid of the container was flushed with nitrogen. No irradiation was carried out before the oxygen level, which was measured with an oxygen indicator from the Orbisphere company, was well below 100 $\mu g l^{-1}$ (mostly around 20 $\mu g l^{-1}$)in the cooling tank [23]. The de-gassing was also maintained during the irradiations and the oxygen level was continously observed.

4. Preparation of the biological material

For the initial experiments carried out, three beans were "fixed" immediately after irradiation, referred to as time T_0. Thereafter three beans were fixed in time intervals of 2 hours up to 14 hours

after irradiation and then again at 24,30,36,42,48,60 and 72 hours. In later experiments between 5 and 7 beans were fixed only at 24,30, 36,42 and 48 hours after irradiation. The reason for this will be given in the result section. In this content "fixing" a bean means breaking about 3 cm off the root tip and immersing it in a liquid consisting of acetic acid and ethyl alcohol in the ratio of 1 to 3. The tubes containing the beans are marked with the information of radiation quality, dose, dose rate, fixation time (time after irradiation) and the real time. The beans are left in this fixative for 3 hours after which they are transferred to 70% ethyl alcohol. Later the beans are transferred again, this time to preservative mixture which consists of:

i) 70% alcohol

ii) acetic acid (concentrated)

iii) 50% glycerol (1/2 glycerol+1/2 absolute alcohol)

in a ratio of 2:1:1. The beans remain stable for several months in this solution.

The staining has been carried out, following the procedure described by John R.K.Savage [46] using Feulgen reagent; the permanent mount of the preparation (slide) was made using the dry ice method [47]. These slides containing the cells of the first 1,5 mm of the root tip are now ready to be analyzed with the microscope.

5. Mathematical analysis of the experimental data

For each fixation point 3-5 slides are available and each slide contains the meristematic cells of one bean. 1000 cells are scored per slide to determine the amount of cells with micronuclei, the number of micronuclei and the mitotic index. Those 1000 cells have been divided into 10 subgroups containing 100 cells. From these data the mean value μ and the variance s^2 have been calculated, where μ, the

mean value, is given by :

$$\mu = \frac{1}{l} \sum_{j=1}^{l} x_j$$

and s^2, the variance, is calculated from:

$$s^2 = \frac{\sum_{j=1}^{l} (x_j - \mu)^2}{l-1}$$

where l = number of subgroups per bean, which is here ten (10* 100 cells were counted per slide).

From the 3-5 slides per fixation point the sample mean at this particular time interval can be calculated and the resulting variance is then determined by the weighted variance [48]. This weighted variance is calculated from the variance of the distribution of each slide found from:

$$s^2 = \frac{s_1^2 (n_1-1) + s_2^2 (n_2-1) + \ldots + s_k^2 (n_k-1)}{n-k}$$

with :

$$n = \sum_{i=1}^{k} n_i$$

s_1, s_2, ..., s_k are the variances of the beans per fixation point; n_1, n_2, ..., n_k stands for the sample size and k is equal to the number of beans per fixation point.

Taking as example only 3 slides this will reduce in our case to:

$$s^2 = \frac{9s_1^2 + 9s_2^2 + 9s_3^2}{30 - 3}$$

from which follows:

$$s^2 = \frac{s_1^2 + s_2^2 + s_3^2}{3}$$

As will be explained in the result section a good estimate of the damage produced by radiation is achieved by using the mean value of

the number of micronuclei and the number of cells with micronuclei found between 24 and 48 hours after irradiation. The final mean value for micronuclei induction and for the mitotic index was then determined, and the final variance for each irradiation dose was calculated by using the error propagation method [49]. From this the standard error of the mean can be calculated :

$$SE = \sqrt{\frac{s^2}{1}}$$

CHAPTER V

DOSIMETRY

The absorbed dose D, is defined as the quotient of dε by dm, where dε is the mean energy imparted by ionizing radiation to the matter in a volume element and dm is the mass of the matter in that volume element. The unit of the absorbed dose was until recently the rad, now it is the Gray.

1Gy = 100 rad

1cGy = 1 rad

1Gy = 1 J/kg

This dose can be measured with ionization chambers by using the Bragg-Gray principle. If a beam of photons traverses a medium into which a cavity has been introduced, the ionization produced in this cavity can then be related to the energy absorbed in the medium by the Bragg-Gray formula.

$$E(m) = S(g,m) * W(g) * J(g)$$

Here E(m) is the dose in the medium measured in Gray. J(g) is the measured ionization per gram of air in the cavity - that is, the ion pairs per gram of air and W(g) is the average energy in J needed to produce an ion pair. The corresponding dose in the medium is then found by multiplying this value by S(g,m), the effective stopping power ratio. This value is needed because different materials are ionized to different degrees by the same energy γ-rays striking them. As a result, a γ-ray of a given energy produces a different number of

electrons in the gas than it would when traversing an equal mass of tissue. S(g,m) expresses the ratio between these numbers [50].

The energy loss of a particle of kinetic energy E(kin) along its trajectory is given by the Bethe-Bloch formula:

$$\frac{dE}{dx} = \frac{4\pi e^2(ze)^2}{mv^2} nZ \left[\ln\frac{2mv^2}{I} - \ln(1-\beta^2)-\beta^2\right]$$

where: m=electron mass; v=velocity of the particle; ze=charge of the particle; n=the number of atoms per cm^3; Z=atomic number; I=the ionization potential of the material; $\beta=v/c$.

This energy loss depends mainly on the charge and kinetic energy of the particle. Because this energy is transferred to the surrounding medium, dE/dx is also referred to in radiobiology as the Linear Energy Transfer (LET). Particles such as α or d-particles or slow protons lose a large amount of energy per unit path length when they traverse a medium. Therefore they are called high LET particles.Electrons or γ-rays which lose only relatively little energy are called low LET particles.

1. Interactions of γ-rays with tissue and their dosimetry

The gamma rays from the ^{60}Co-gamma source are produced after β-decay from the de-excitation of the newly formed ^{60}Ni nuclei at energies of 1.17 MeV and 1.33 MeV (fig.25).

The absorption of 60-Co gamma rays in tissue is almost entirely by Compton recoil, producing electrons of all energies from zero up to about 1.3 MeV. However, most of the electrons will have an energy between 0 and 100 keV. After several Compton interactions the energy of the gamma will be so low that its residual energy will be given to a photo electron.

All gamma irradiations have been carried out with a 10 Ci ^{60}Co-gamma source, located in the irradiation room at the CERN cali-

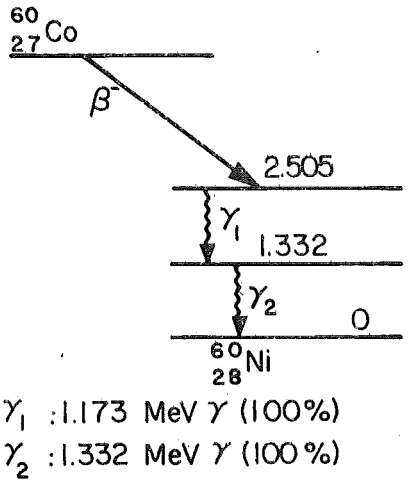

Figure 25: The decay scheme of ^{60}Co-gamma.

bration facility. The source is operated by a remote control system. In the extracted position the source is surrounded by a 16 cm diameter lead collimater into which a beamshaper can be introduced. In all the experiments reported here the so called wide beam shaper which could produce a beam of 48cm width at a distance of 1m was used. The dose rate measurements were carried out with a 0.1 cm^3 EGG ionization chamber(216-56).The EGG chamber was inserted in a water tight plexiglas tube and fastened on a scanner.The measurements were made at 4 different water depths in the bean tray. A vertical scan of the dose rate distribution in Pos.2, the irradiation position of the beans, was made around the center. In this way an irradiation region was determined where the dose rate did not vary more than ± 4%. This region was then marked on the net of the bean holder and great care was taken that all the bean meristems were within this region. The roentgen obtained from the Baldwin Farmer chamber was converted to absorbed dose after correcting for temperature and pressure fluctuations [51]. A dose rate of about 500 cGy/h was obtained when the distance between collimator and irradiation container was 20 mm. At a distance of 130 mm the dose rate was about 150 cGy/h.

2. Interactions of neutrons with tissue and their dosimetry

Neutrons entering a biological medium release energy by different types of strong interactions; namely: (1) elastic scattering, (2) inelastic scattering, (3) nonelastic reactions, (4) capture processes, (5) spallation reactions.

(1) elastic scattering

When a neutron is scattered elastically by an atom, energy is transferred to the nucleus. Of the four most important elements in tissue : oxygen, carbon, hydrogen, and nitrogen, the elastic cross sections are all generally decreasing with increasing neutron energy.

(2) inelastic scattering

Inelastic scattering refers here to (n,n′) reactions (eg. $C^{12}(n,n'\gamma)C^{12}$) in which the neutron interacts with a nucleus but is promptly re-emitted, generally with a changed energy and direction. Most reactions of this type are accompanied by the emission of a nuclear de-excitation γ ray. Inelastic scattering begins at a neutron energy of about 2.5 MeV and becomes important at an energy of about 10 MeV.

(3) nonelastic reactions

In nonelastic reactions the struck nucleus emits particles other than a single neutron (eg. $O^{16}(n,\alpha)C^{13}$ or $N^{14}(n,t)C^{12}$) All cross sections for nonelastic processes become significant at neutron energies greater than 5 MeV and increase generally as the neutron energy increases to about 15 MeV. Although most of these reactions are accompanied by de-excitation γ-rays, the proton and α-particle producing reactions are more important in view of this work, because of the high LET of these particles and because of the total absorption of their energies near the reaction site. At neutron energies greater than 20 MeV, nonelastic cross sections contribute an increasing fraction of the total dose because of the increased average energy of the

particles produced by the interaction.

(4) capture processes

Capture processes are not very important in the range of neutron energies studied in this work. The only reactions which are contributing to the dose in soft tissue are the ${}_1H^1(n,\gamma){}_1H^2$ and ${}_7N^{14}(n,p){}_6C^{14}$ reactions, and then, only in the thermal or near thermal energy region.

(5) spallation reactions

Spallation is a process where a nucleus is fragmented, ejecting several particles and nuclear fragments . From an energy of about 20 MeV upwards this reaction starts to be significant for the C,N and O elements. The cross section curve rises slowly with increasing neutron energy to about 400 MeV and then becomes nearly constant. Most of the energy released is by heavily ionizing fragments, so that the locally deposited energy is rather high.

At energies above 290 Mev pion production starts.

2.1 SC-neutron beam dosimetry

The neutron beam is produced by 600 MeV protons incident on a 10 cm thick beryllium target at the CERN Synchro-Cyclotron (SC). The secondary neutrons are then extracted in the forward direction and pass down a 6 m long collimator, through the cyclotron shielding wall (fig.26). The incident protons and the secondary charged particles are bent out of the neutron beam by two sweeping magnets located before and after the collimator. The distance between production target and irradiation position is 12.5 m and the diameter of the collimator is 10 cm. The energy spectra of the secondary neutrons is expected to be rather broad with a maximum energy equal to the initial 600 MeV proton energy and a peak maximum at about 50 MeV below the incident energy [52,53]. Because only the charged particles are

removed from the neutron beam, there will be a contamination of gamma rays in the beam, which come primarily from the decay of neutral pions produced in the proton-target interaction. These gamma rays have a broad energy spectrum with maximum emission of around 100 MeV [54].

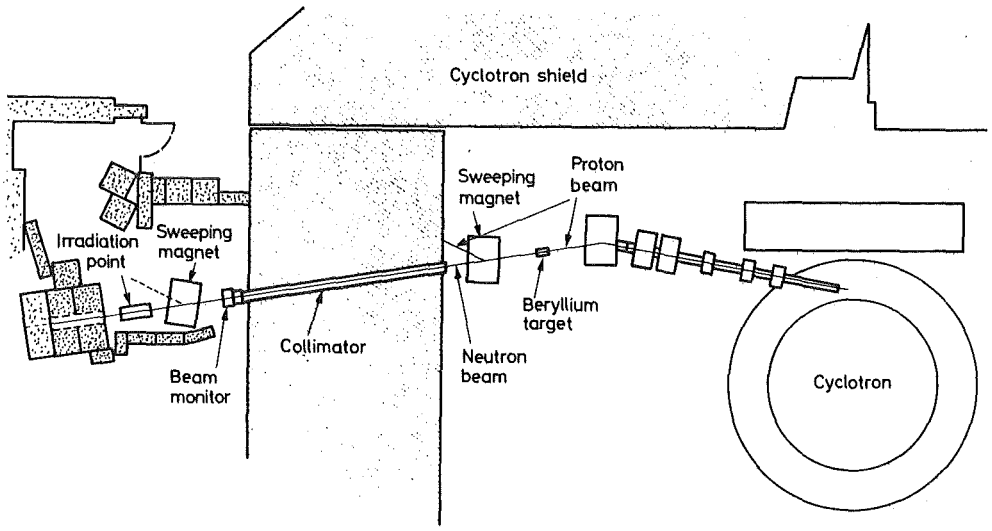

Figure 26: The experimental area of the SC.

The useful beam diameter at the irradiation point, where the intensity varied by less than 5%, was 14 cm. The flux density of neutrons below 20 MeV in the pure beam was estimated to be 1.1×10^5 n/cm^2/sec from the activation of indium foil inside a 15 cm diameter polythene moderator covered with cadmium [55]. In comparison the beam intensity of the higher energy neutrons was 10^6 n/cm^2/sec as measured from the activation of carbon-11 in a plastic scintillator. The reaction $^{12}C(n,2n)^{11}C$ has a threshold at about 20 MeV and the cross section stays reasonably constant at 22 mb up to high energies [56]. The contribution of gamma rays to the dose was estimated by exposing an unfiltered X-ray film. This film, which has been calibrated with gamma rays from the ^{60}Co -gamma source, is even more sensitive to high energy gammas and it is assumed that the effect of the neutrons is very small. The actual contribution will therefore be slightly

overestimated and the upper limit of the gamma ray contribution at an absorber depth of $1 g/cm^2$ was therefore determined to be about 10% of the total dose [57].

The dose rate was measured with a parallel-plate tissue equivalent ionization chamber, as well as with a 0.1 cm^3 tissue equivalent chamber in a water absorber and with a 1 cm^3 spherical chamber in a tissue- equivalent plastic absorber. It builds up rapidly with penetration in an absorber due to the production of secondary charged particles (fig.27).

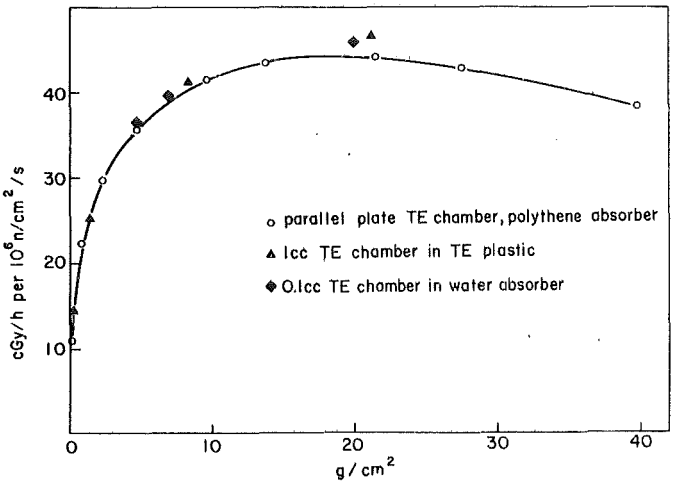

Figure 27: The dose rate build up as a function of water depth.

Tissue equivalent chambers are normally used because the dose determination is simplified if the surrounding medium has the same composition as the chamber. The tissue equivalent material developed by Shonka consists of 10.1% H, 3.5% N, 86.4% C and traces of oxygen. The tissue equivalent gas with which the ionization chamber is filled has the following composition: 64.4% CH_4, 32.4% CO_2, 3.2% N_2. However, tissue equivalent material has an excess of carbon, whereas tissue contains more oxygen. The dose estimations at a given absorber depth were carried out with a tissue equivalent ionization chamber filled with tissue equivalent gas, which had been previously calibrated with ^{60}Co-gamma rays. The dose rate is obtained from the ionization current produced in the chamber by the relation:

$$D = S\ f_1\ f_2\ i/p\ (Gy/h)$$

where S is the sensitivity of the chamber determined from calibration with a known ^{60}Co-gamma source, i is the output current measured in picoamperes, p is the absolute gas pressure in kg/cm^2 at 20^0C and f_1 is a correction factor to allow for the slight tissue inequivalence of the chamber when compared to soft tissue, overestimating the dose by about 5% [58]. f_2 is a correction factor which takes into account the efficiency of the chamber and includes recombination losses and variation of the energy required to form an ion pair. The biological experiments were all carried out at a water depth of 0.25 g/cm^2. Here the contribution to the dose from nuclear interactions is dominant. The dose rate variation in this region is shown in figure (28).

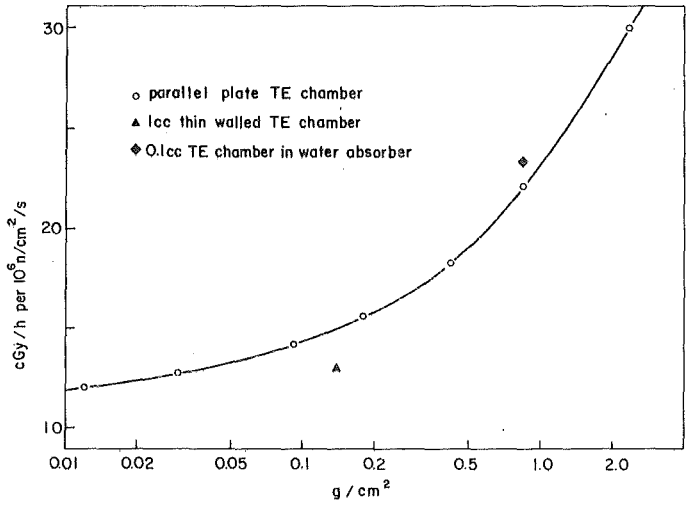

Figure 28: The dose-rate build up in the first 0.25 g/cm^2.

An estimation of the contribution of backscattering to the dose was made by reversing the thin walled parallel-plate ionization chamber, so that its window was facing down the beam and adding backscatter material. The contribution of the backscattering to the dose measured at a water depth of 3 g/cm^2 was about 8%.

The energy spectra of the secondary protons was measured using a counter telescope [59]. From these results the absorbed dose in different materials, eg. water, carbon and lucite was determined and

compared with the total dose measured using an ionization chamber. The results showed that the largest contribution to the absorbed dose comes from secondary protons which is in close agreement with the calculations made by Alsmiller et al.[60].

2.2 ^{252}Cf-neutron dosimetry

The ^{252}Cf-neutron source emits neutrons by spontaneous fission. Its half life is 2.65 years. The effective neutron output on the day of irradiation was 1.62×10^{8} n/sec. It is the spontaneous fission that results in the mixed neutron-γ-ray emission. The mean energy of the fission neutrons is 2.35 MeV (see fig.29), and most of the gamma rays are produced with energies up to about 1 MeV (see fig.30) [61].

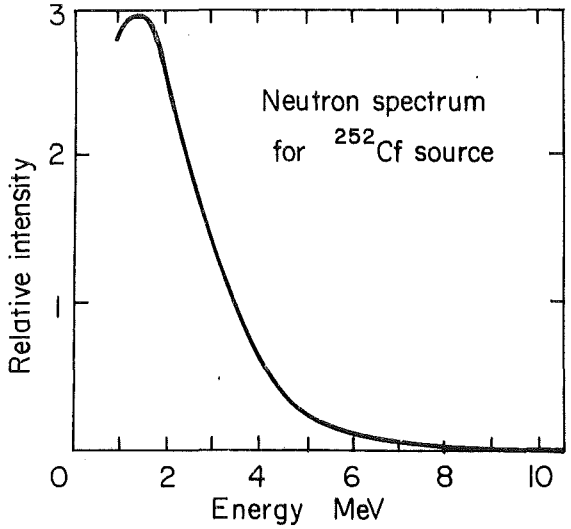

Figure 29: The fission neutron energy spectra.

Figure 31 indicates the positions where dose rate measurements were carried out. At positions A_1-A_2-A_3-B_1-B_2-B_3 the dose rate dependence on the radial distance from the source was measured at distances of 60,70 and 80 mm respectively. In addition, at position A_1, the dose rate as a function of height in the tank was determined. Furthermore, a comparison was made between the reading of an air filled and a tissue equivalent gas filled chamber, showing an 11.6% higher value in the case of the TE-gas filled ionization chamber. All measurements made with the air filled chamber were corrected for this

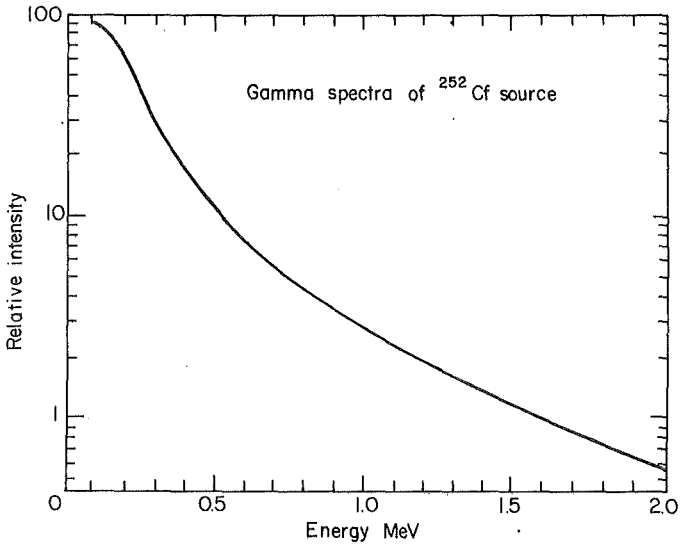

Figure 30: The gamma ray energy spectra.

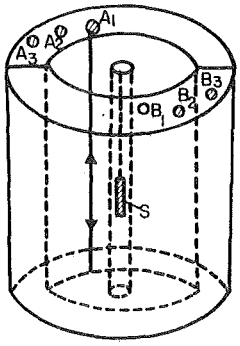

Figure 31: The positions were the dose measurements were carried out.

difference. The gamma contamination was determined with a Geiger-Mueller counter. The measurements gave a total dose rate of 7.0 ± 1.0 cGy/h in the position of the bean irradiation. The gamma dose rate was 2.9 cGy/h and the neutron dose rate was 4.1 cGy/h. In addition an indium activation measurement was carried out to determine the neutron flux. The mean value determined from several measurements was : $F = 4.5 \times 10^5$ n/cm^{-2}/sec^{-1} . From this the neutron dose rate can be determined by using the neutron kerma value of $3.0 * 10^{-9}$ cGy/n/cm^2 [62].

$$D = F \times 3.0 \times 10^{-9} \times 3600 \text{ (cGy/h)}$$

$$D = 4.86 \text{ (cGy/h)}$$

This value is rather comparable with the dose rate of 4.1 cGy/h as

determined by the ionization chamber measurements.

3. Interactions of pions with tissue and their dosimetry.

Pions are produced in nucleon nucleon interactions when the energy in the lab-system exceeds 290 MeV. Charged pions with a kinetic energy E(kin) are slowed down when passing through matter by ionization losses. The slowing down region is also called the plateau region. In this region the main interaction with matter is via ionzation even if some nuclear reactions are also taking place.

If the negative pion has no kinetic energy left it is soon captured into a high circular Bohr orbit from which it starts to cascade down to the K-shell. These orbits have much smaller radii than the electron orbits because of the larger mass of the pion (280 times the electron mass). The π-mesic X-rays associated with transition in these orbits are also of corresponding larger energies (5 MeV or more) . Eventually the negative pion is captured by the nucleus. If a "star" event occurs, one or more charged particles are expelled from the nucleus. The large amount of energy released by the capture process makes it also possible that the nucleus breaks up into α-particles, deuterons and protons. In the cases where no star event occurs only neutral particles are expelled (eg. one or more neutrons carry off all the energy). This stopping region is also called the Bragg-peak. In addition to the secondary particles there will be a relatively large contamination of muons in the pion beam, because the lifetime of a negative pion is only $2.6*10^{-8}$ seconds and it will therefore quite frequently decay in flight into a muon and a neutrino [54]:

$$\pi^- \rightarrow \mu^- + \nu + 34 \text{ Mev}$$

The experiment involving pions has been carried out at SIN (Schweizerisches Institut fuer Nuklearforschung) with the biomedical

(π-E-3) beam. The pions are produced in the collision of 590 MeV protons with a beryllium target. This pion beam is then bent down vertically into the biomedical irradiation cave. Along the 10.7m long beam line are several quadrupole lenses, bending magnets and collimators. These elements can be adjusted to optimize the intensity, the intensity distribution, the momentum, the momentum distribution and the beam size. The mean momentum of the beam was 172 MeV/c. The momentum distribution itself could be varied by opening or closing the slit situated between the two bending magnets inside the QSK 72 lens (fig.32). For this experiment the width of the slit was 65 mm which gave a momentum spread of 13.9 MeV/c FWHM (Full Width Half Maximum) [63]. The focusing of the beam was made with the last lenspair providing a circular beam. The intensity distribution had a FWHM of 6cm at 1m above the floor, ensuring a uniform dose distribution over a diameter of about 2cm. The beam was monitored with a thin-walled transmission ionization chamber mounted on the end of the beam pipe. The beam shape was determined in air at five positions along the beamline with X-ray films. The profile was measured with a $1cm^3$ spherical tissue equivalent chamber.

All the dose rate measurements were carried out at the irradiation point. The dose rate was measured with a parallel plate chamber with a collector electrode of 25 mm diameter and a single gap of 2 mm. The volume of the chamber is small enough to be located at well defined positions. The material surrounding the sensitive volume was made of the tissue equivalent material already described and was of sufficient thickness that the ionization due to secondaries generated in the plastic could be considered to be in equilibrium in the chamber [64,65]). As has been calculated by Dutrannois et al.[66], 95% of the charged particle energy coming from pion capture in oxygen or carbon is absorbed within a depth of 3 g/cm^2 of water.

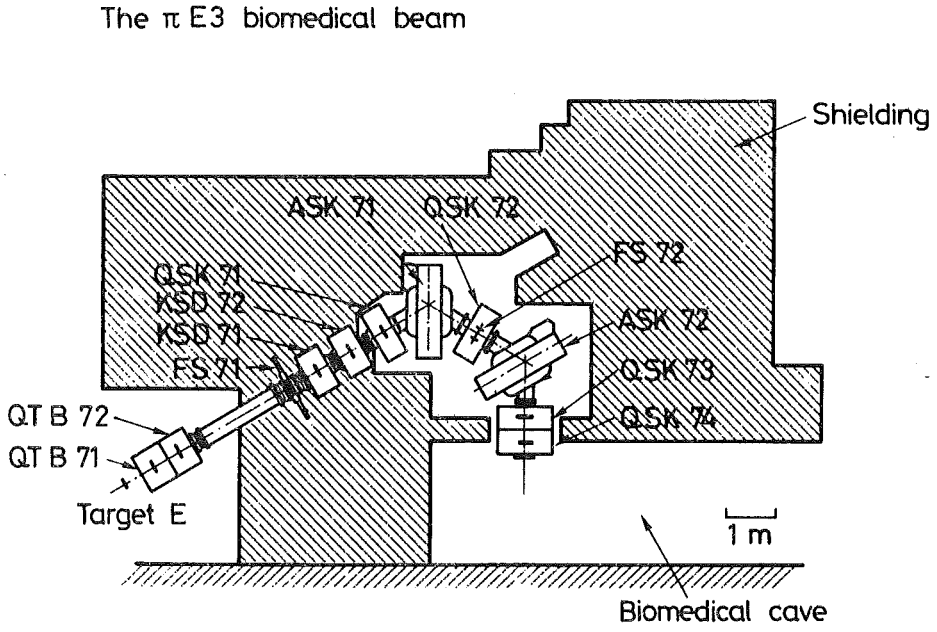

Figure 32: The beamline of medical beam.

There will be an over-estimation of the dose by about 8% due to the difference in pion interaction products from the oxygen of tissue [67] and carbon, which has been shown already to be the major constituent of the chamber. The over all uncertainty in the dose estimation will be about 5% [68].

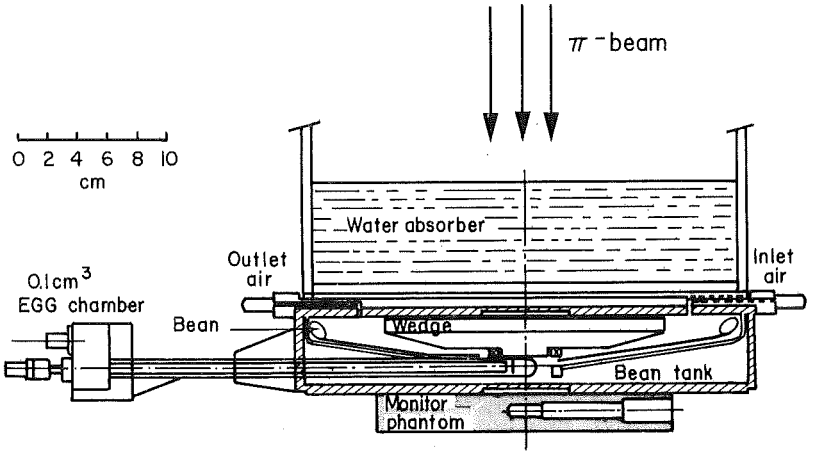

Figure 33: Experimental set up for negative pion irradiation.

Above the ionization chamber a water tank was located (fig.33) which could be filled and emptied via a remote control system. In this way the dose rate as a function of water depth could be measured (fig.34). As can be seen from this figure the range of the pions is

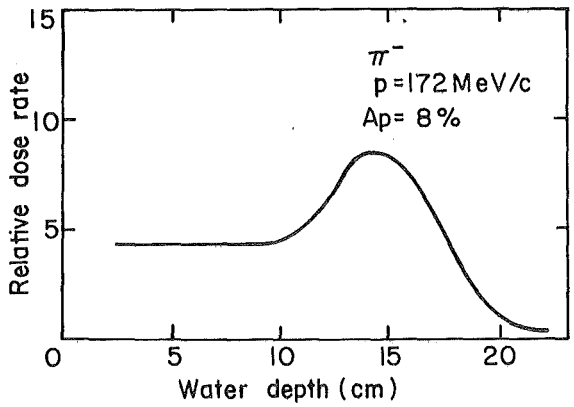

Figure 34: The negative pion dose-rate as a function of water depth.

about 20 cm in water. Because of the relatively large momentum spread used the Bragg peak is rather broad.

The stopping rate of the pions in the irradiation position had been determined by B.Nordell et al.[64] using a counter telescope .

A very thorough investigation of the energy spectra of secondary particles emitted after the absorption of stopped negative pions in different chemical elements has been carried out by a group from the Nuclear Research Center in Karlsruhe at SIN [69,70, 71,72,73,74,75,76]. Their results showed that by far most of the secondary particles produced were neutrons with energies betweeen 0.5 and 100 MeV. They were followed by protons of about the same energy range which were lower by a factor of 5. Alpha particles with energies below 20 Mev were also significantly produced.

The dose deposited by secondary particles in a tissue equivalent phantom has then been calculated using a Monte Carlo program. The results showed that the contribution of secondary neutrons to the dose was even slightly higher than the contribution from all secondary charged particles.

CHAPTER VI

RESULTS

The acentric fragments produced by the radiation will form micronuclei and will be visible after the first mitosis following irradiation. Because the cells in a root meristem are asynchronous and therefore distributed over all cell cycle phases, the first cells containing micronuclei will appear about 4 hours after irradiation. The first micronuclei are the result of chromatid aberrations produced at the end of the G_2-phase. The last micronuclei produced during the first cell cycle should appear about 24 hours after irradiation (equal to the duration of the cell cycle) provided that the cell cycle duration is not prolonged by the irradiation. These are then formed from chromosome aberrations produced at the beginning of the

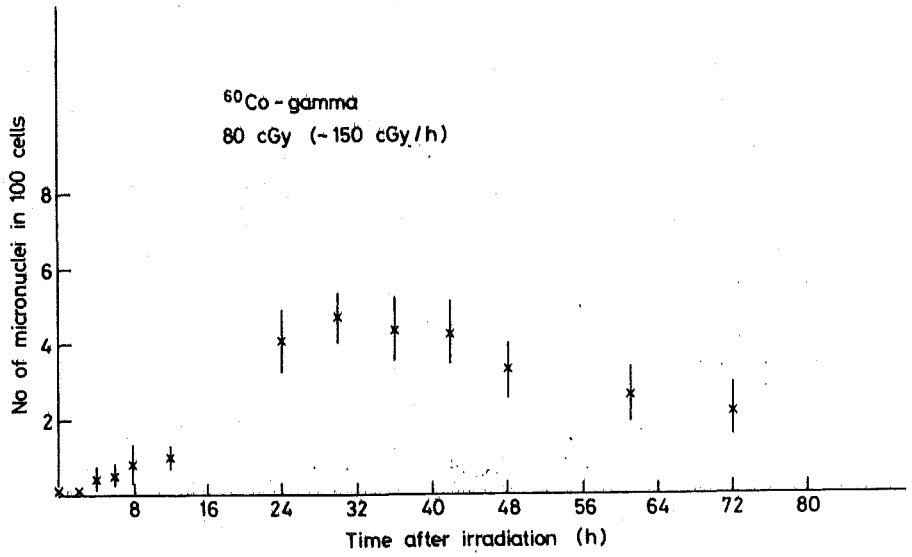

Figure 35: The micronuclei distribution as a function of time after irradiation (80 cGy; 150 cGy/h).

G_1-phase. An example of the appearance of micronuclei after irradiation is given in figure (35). As can be seen there is a steady increase in the number of micronuclei appearing with time after irradiation. They reach a maximum at about 24 hours and stay on a plateau for about another 24 hours, then their number decreases again. This decrease is mainly due to the fact that cells containing micronuclei are no longer able to survive after such severe damage has been produced. Another reason for this decrease could be the dilution effect produced from cells coming in from the second post irradiation mitosis. However, since half of the newly produced cells will differentiate and become elongated cells, it seems rather unlikely that the dilution effect is contributing very much to this decrease.

To establish a dose response curve which would quantitatively be representative of the damage induced, it was decided not to use either a single fixation point or the cumulative incidence from 0-24 hours after irradiation, as has been done in literature (77,27,78). In the first case the large fluctuations in the appearance of micronuclei observed at high doses would be a source of error (79,80). In the second case, this test might not be sensitive enough at low doses because at fixation times soon after irradiation the number of micronuclei produced is relatively small.

The fact that the cell cycle time of Vicia faba is about 24 hours and micronuclei are visible for at least one cell cycle, produces between 24 and 48 hours a relative stable number of micronuclei. It was therefore decided to use the mean value of micronuclei of this time period as a quantitative estimate of the damage produced. Normally 5 points, each representing at least 3 times 1000 cells, are measured at 24,30,36,42 and 48 hours after irradiation. From these values a mean value is calculated and plotted over dose.

It is possible that when a cell has been heavily damaged not only one but several micronuclei are produced. Therefore each slide was analyzed both according to the total number of micronuclei visible and also to the total number of cells with micronuclei (one or more).

1. Single dose exposures

1.1 SC-neutron results

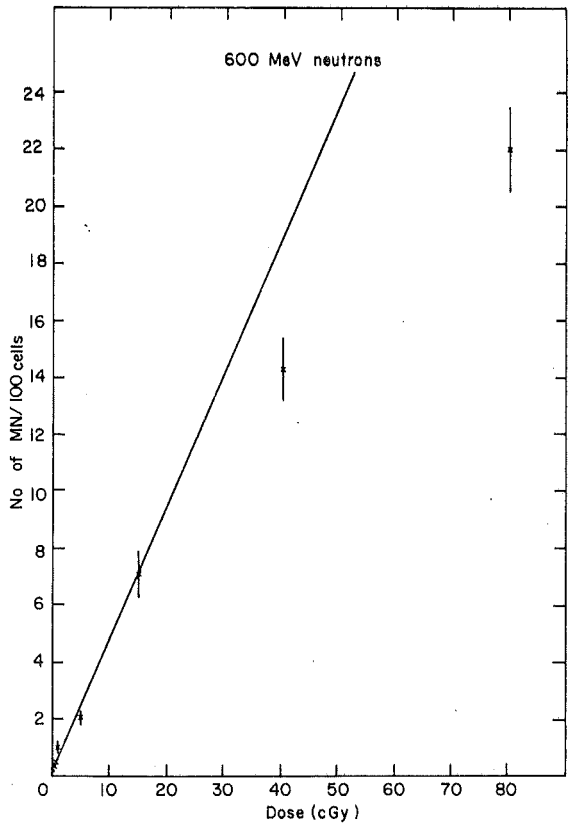

Figure 36: The mean number of micronuclei between 24 and 48 hours plotted over neutron dose (uncorrected data).

The neutron results were obtained during two different experimental periods. During the first experiment the beans were exposed to 1,5,15,40 and 80 cGy. The results indicated that it would be possible to "see" even lower dose effects. A second experiment was done in 1980 when, in addition to a split dose irradiation, single doses of 40 cGy, 0.5 cGy and 0.2 cGy were administered. The data from the single dose exposure will be presented first. In figure (36) the

mean number of micronuclei found between 24 and 48 hours after irradiation per 100 cells scored is plotted over dose. If one tries to fit the data points to a straight line one realizes that the curve starts to bend over above 15 cGy. The reason for this sub-linear increase is the drastic reduction in the mitotic figure at high doses. Because cells have first to go through mitosis before a micronucleus can be formed, a decrease in the mitotic index will then be reflected by a reduction of the number of micronuclei.

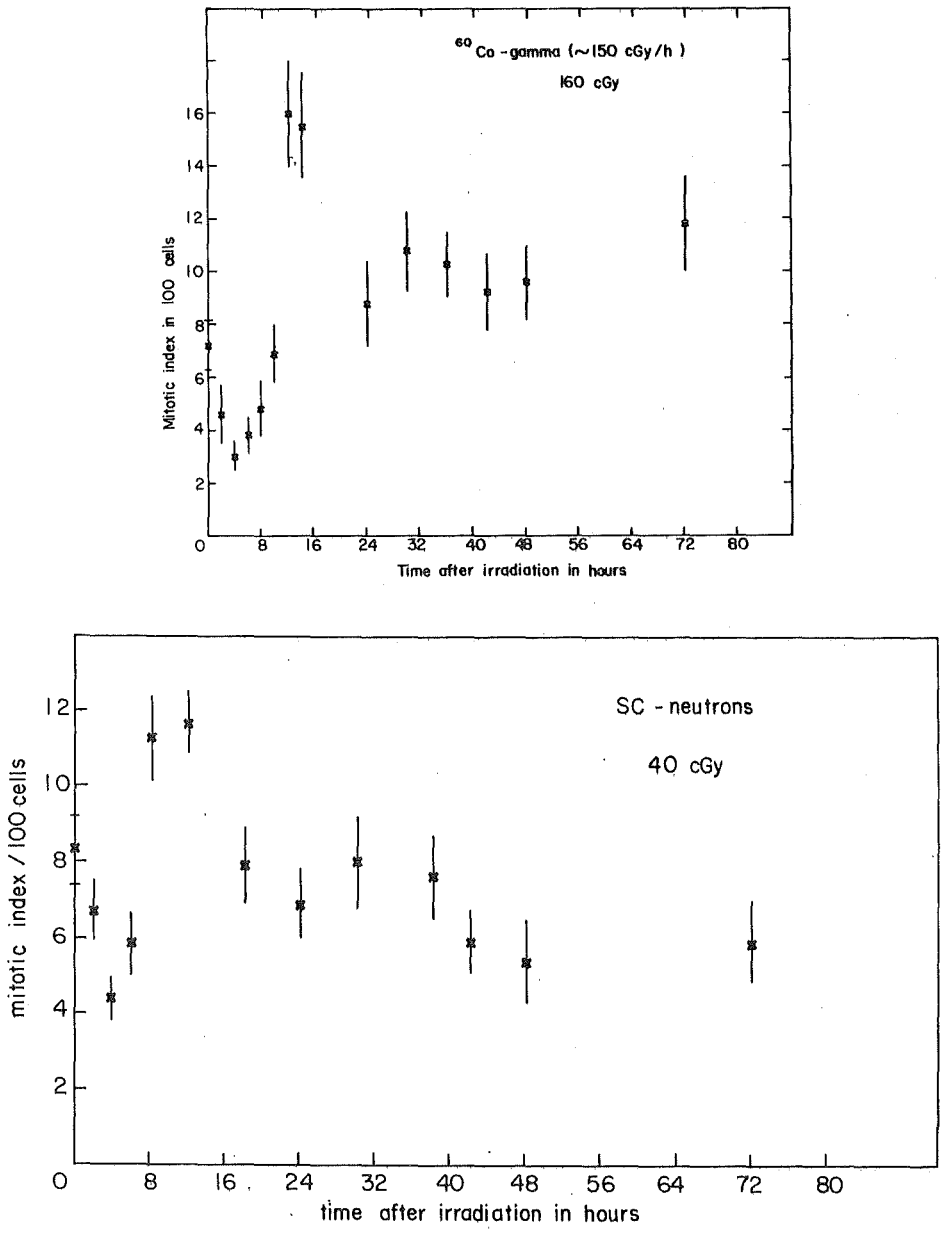

Figure 37: The mitotic index distribution as function of time after gamma and neutron irradiation.

In figure (37) an example of the mitotic index distribution is given. Shortly after irradiation at T=0, the mitotic index drops rapidly reaching a minimum between 4 and 6 hours, followed by a maximum between 12 and 14 hours and then stabilizing after about 24 hours. This oscillation is ascribed to the G_2 blockage produced by the irradiation, which inhibits cells from entering mitosis for a certain time period and which therefore causes the initial drop of the mitotic figure and the subsequent rise. After 24 hours most of the cells have entered the second cell cycle and the left over fluctuation is minimal. Depending on the dose and the radiation quality used, this stabilized mitotic index can be much lower than the corresponding value of the control group. The percentage mitotic index determined from the ratio of the mitotic index between 24 and 48 hours after irradiation to the equivalent one from the control is plotted as a function of dose in figure (38). It can easily be seen that there is a strong decrease in mitotic index in the high dose range (about 40%). There are two possible explanations for this reduction. One is that cells are killed before reaching the first mitosis and the other is that there is a drastic prolongation in cell cycle time. However, interphase death is not very often observed, especially in plant systems [81], and a lengthening in cell cycle time seems therefore more likely. In order to see a drop in the mitotic index rate from a cell cycle prolongation a part of the cycle will have to be unproportionally prolonged.

If one compares the micronuclei distribution after a neutron dose of 15 cGy (fig.39), where only a minor reduction in mitotic index is observed, with the one of 80 cGy (fig.40) one observes no drop in the number of micronuclei after 48 hours with the high dose radiation. Furthermore, the mitotic index distribution for the neutron data at high doses seems to be disturbed. When comparing the distribution

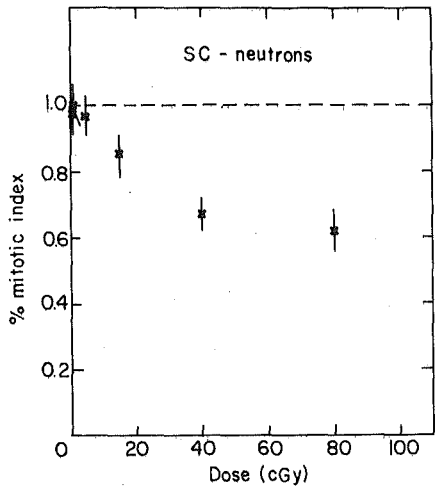

Figure 38: The percentage mitotic index as a function of neutron dose.

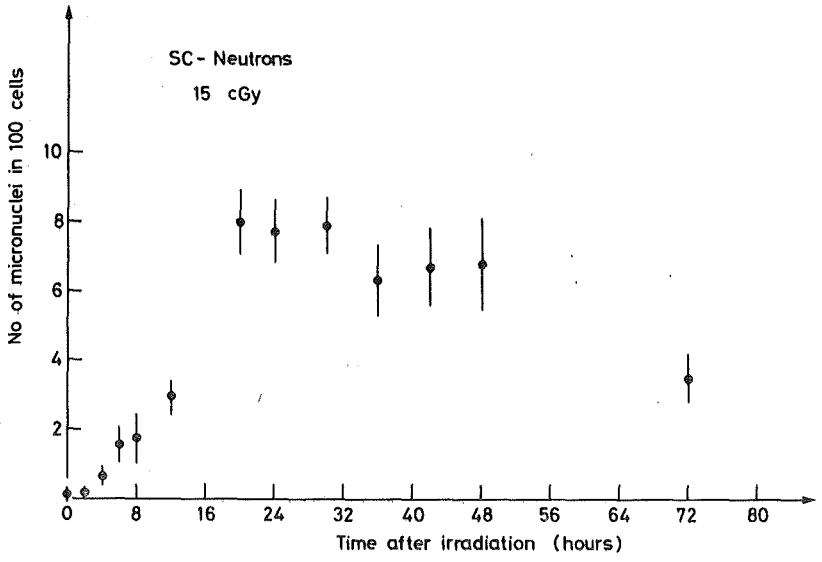

Figure 39: Micronuclei distribution after a neutron dose of 15 cGy.

normally observed for gamma radiation (fig.37) with the one for 80 cGy neutrons (fig.41) one realizes that the maximum is shifted by about 6 hours. Similar delays in cell cycle progression, especially after high LET radiation, have been reported by several authors [82,83,84,85,86]. In our case this lengthening of cell cycle time implies that at high doses more time is needed (more than 24 hours) for the accumulation of cells containing micronuclei. Normalizing the experimental data for micronuclei by dividing by the percentage mitotic index takes this problem into account, and a curve which is

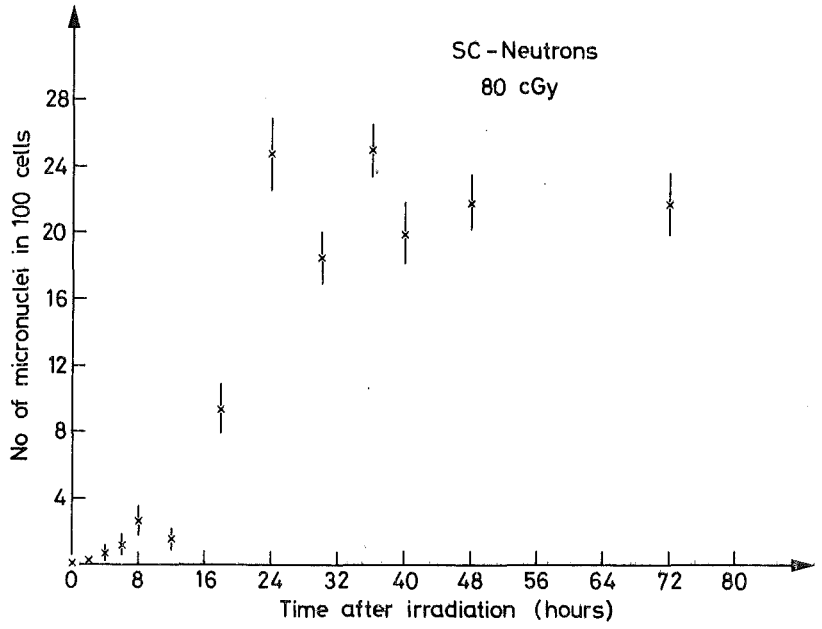

Figure 40: Micronuclei distribution after a neutron dose of 80 cGy.

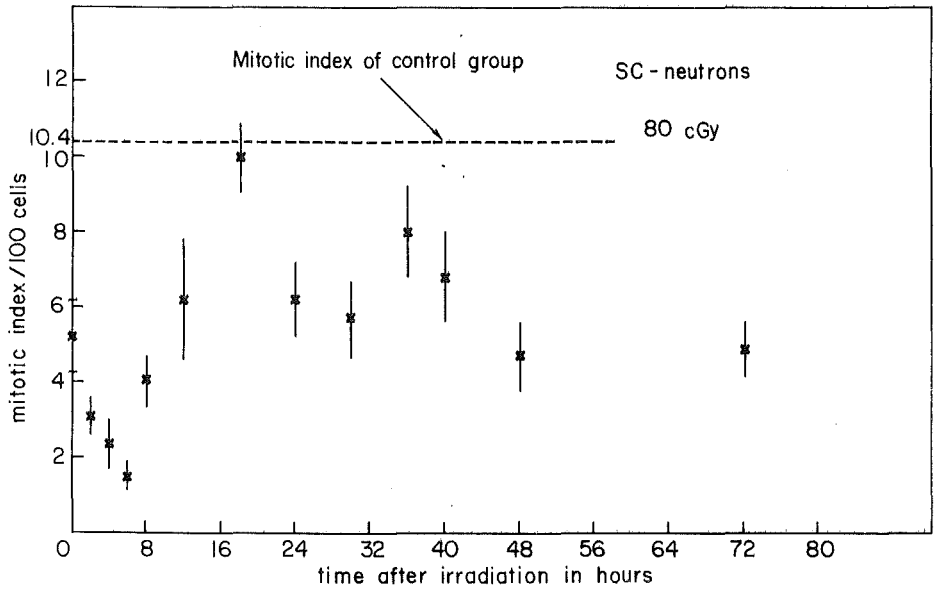

Figure 41: The mitotic index distribution after a neutron dose of 80 cGy.

well fitted by a linear equation is then obtained(see fig.42). From now on the experimental data will be presented in the table, whereas the figures will contain the "corrected data". The data have been fitted to the linear equation : $E = C + \alpha D$, using the Minuits program available in the CERN Program Library. The chi-square value divided by the degrees of freedom for this weighted linear least

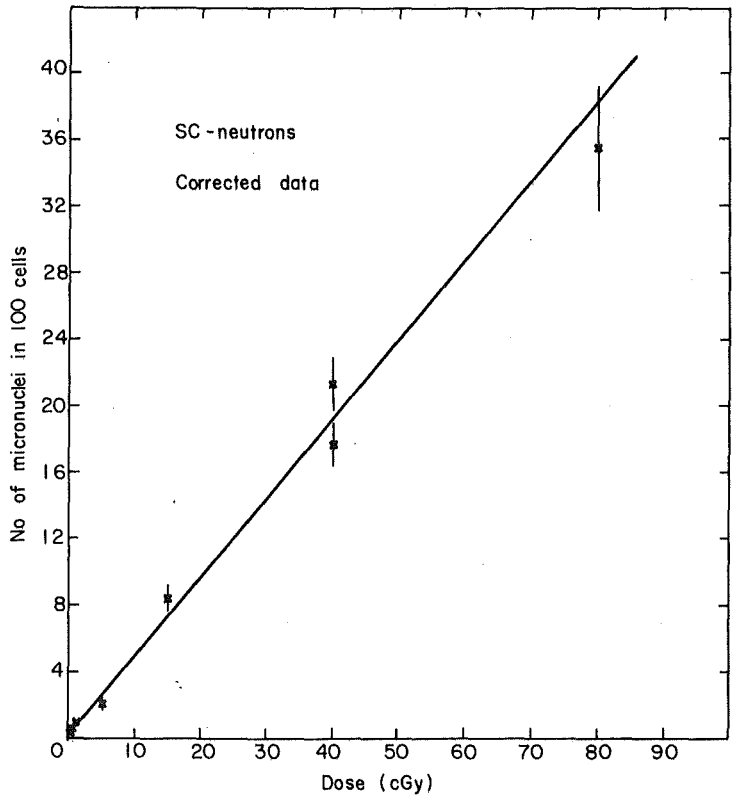

Figure 42: Corrected number of micronuclei as a function of neutron dose.

square fit (LSQ) was : $\chi^2/f = 1.9$. The coefficients were found to be : $C = 0.13 \pm 0.04$ and $\alpha = (0.48 \pm 0.02) cGy^{-1}$, where C stands for the number of micronuclei in the control group [87,88].

The experimental data for the number of cells with micronuclei and the corresponding percentage mitotic index for the different doses are given in Table 2. As can be seen from Table 2, the number of micronuclei found for the 0.2 cGy dose is rather similar to the control value. To be sure that the slight difference observed is a "real" effect the number of beans was plotted as a function of the number of micronuclei observed per bean, where 1000 cells were scored per bean (fig.43). The shape of the distribution for the control groups is completely different from the shape of the irradiated groups, thus indicating that the effect, though maybe not statistically significant, is real.

Table 2: The experimental data of the high energy neutron experiments.

Dose (cGy)	Mitotic Index (MI)	No of MN/ 100 cells	No of cells with MN/ 100 cells
$0^{1)}$	9.8±0.5	0.21±0.05	0.21±0.05
$0^{2)}$	11.2±0.6	0.15±0.05	0.14±0.04
$0.2^{2)}$	10.9±0.4	0.19±0.07	0.17±0.06
$0.5^{2)}$	10.9±0.3	0.41±0.11	0.38±0.11
$1.0^{1)}$	10.3±0.4	1.0 ±0.2	0.9 ±0.2
$5.0^{1)}$	9.5±0.4	2.0 ±0.2	1.8 ±0.2
$15.0^{1)}$	8.3±0.4	7.1 ±0.5	6.4 ±0.4
$40.0^{1)}$	6.6±0.4	14.3 ±0.6	12.6 ±0.5
$40.0^{2)}$	8.3±0.7	13.1 ±1.0	11.2 ±0.8
$80.0^{1)}$	6.1±0.5	22.0 ±0.9	18.2 ±0.6

The indices 1) and 2) refer to two separate experiments.

1.2 ^{252}Cf-neutron-results

The linear energy transfer of high energy neutrons is considerably lower than that of neutrons commonly used in radiotherapy, which have energies below 14 MeV. Observing such a strong response after high energy neutron irradiation, it seemed of interest to measure the effect produced by ^{252}Cf-neutrons which have a mean energy of 2.35 MeV. The number of micronuclei, the number of cells with micronuclei and the mitotic index were again determined for doses of 0.2,0.5,1 and 5 cGy. The experimental data are given in Table 3.
The corrected number of micronuclei as function of dose has been fitted to the linear equation : $E = C + \alpha D$ ($C=0.09\pm0.04$; $\alpha=(1.2\pm0.1)cGy^{-1}$),(figure 44). The resulting χ^2/f was found to be 0.4.

1.3 ^{60}Co-gamma-results

The data for the ^{60}Co-gamma rays were obtained from several successive experiments. During the first experiment carried out in May 1978, doses of 160,110,80 and 55 cGy at a dose rate of about 500 cGy/h and two doses, namely 160 and 80 cGy at a dose rate of 150

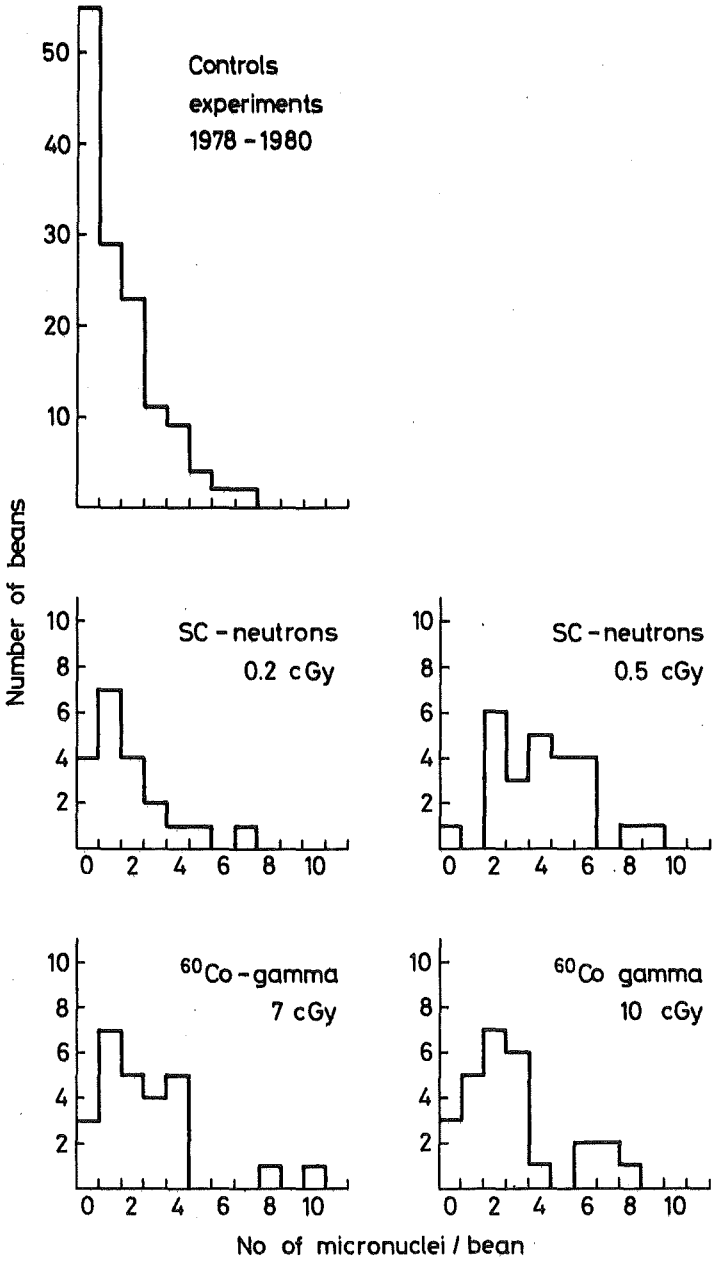

Figure 43: The number of beans as a function of micronuclei.

cGy/h were given. An analysis of the data showed that it would again be possible to investigate the effects of much lower doses. The lowest dose finally administered was 7 cGy. In table 4 the time schedule of the gamma ray experiments is presented. It can be seen that the data for the 150 and 500 cGy/h curves were obtained from many different experiments proving the reproducibility of this system.

Table 3: The experimental data of the ^{252}Cf-neutron experiment.

Dose (cGy)	Mitotic Index (MI)	No of MN/ 100 cells	No of cells with MN/ 100 cells
0.0	9.7±0.4	0.09±0.05	0.09±0.05
0.2	8.8±0.5	0.37±0.15	0.31±0.09
0.5	9.4±0.5	0.62±0.15	0.57±0.12
1.0	9.7±0.6	1.14±0.18	1.08±0.17
5.0	8.9±0.5	5.7 ±0.4	5.2 ±0.3

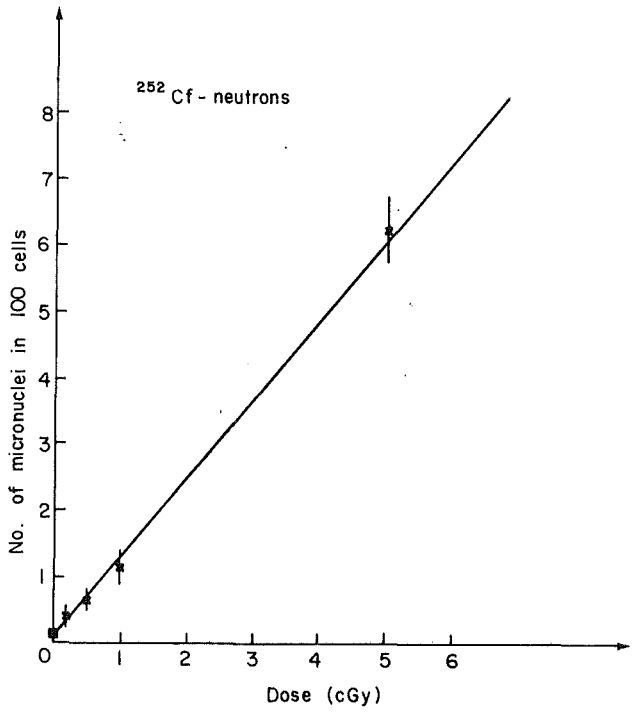

Figure 44: Corrected number of micronuclei as a function of ^{252}Cf-neutron dose.

1.3.1 500 cGy/h and 150 cGy/h experiments

The percentage mitotic index as a function of dose is shown for both dose rates in figure (45). Even at the highest dose the percentage mitotic index did not drop below 80% which is in strong contrast to the drop observed after neutron radiation. In figures (46) and (47) the corrected mean number of micronuclei are plotted over dose for the two dose rates of 150 cGy/h and 500 cGy/h. The data have

Table 4: The time table of the different gamma experiments.

MAY 1978:
500cGy/h: 55,80,110,160cGy, (55+55)cGy and (80+80)cGy 1 hour split dose.
150cGy/h: 80,160cGy

FEB.1979:
150cGy/h: 55,110cGy

JUNE 1980:
500cGy/h: 10,20,190cGy and the (95+95) split dose exp.
150cGy/h: 20cGy

OCT.1980:
150cGy/h: 7,10,15cGy

DEC.1980:
500cGy/h: 40cGy and (20+20) split dose exp.
150cGy/h: 160,190cGy
10cGy/h: 7,10,15,20cGy

been fitted to the following equation : $E = C + \alpha D + \beta D^2$, where E stands for the effect observed, C for the control value at zero dose, α and β are coefficients and D is the dose administered. The χ^2/f-value is 2.9 for the 150 cGy/h curve and 1.9 for the 500 cGy/h curve. The coefficients in the case of 150 cGy/h irradiation are $C=0.12\pm 0.02$; $\alpha=(3.2 \pm 0.2)\ 10^{-2}cGy^{-1}$; $\beta=(2.5 \pm 0.2)\ 10^{-4}cGy^{-2}$. For the 500 cGy/h irradiation they are : $C=0.12\pm0.02$; $\alpha=(1.8\pm0.2)10^{-2}cGy^{-1}$; $\beta=(4.4\pm0.2)10^{-4}cGy^{-2}$.

The experimental values are presented in Table 5.

From figure (48) where the curves of both dose rates have been plotted together, it can be seen that only in the high dose region is a dose-rate effect observed (see also figure 50).

The definition of the shape of the dose-effect curve at low doses being a main question, the experimental points have also been fitted to the following equation : $E = C + \beta D^2$.

In this case the χ^2/f value is 4.7 for the 500 cGy/h curve and 8.6

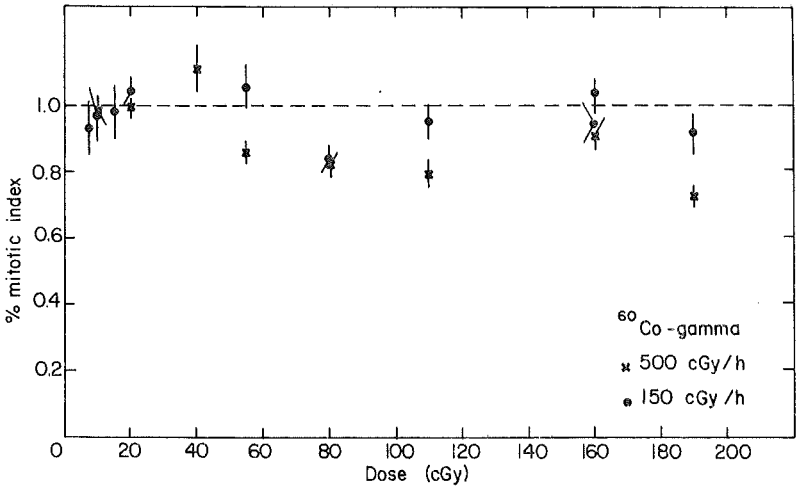

Figure 45: The percentage mitotic index as a function of γ-ray dose.

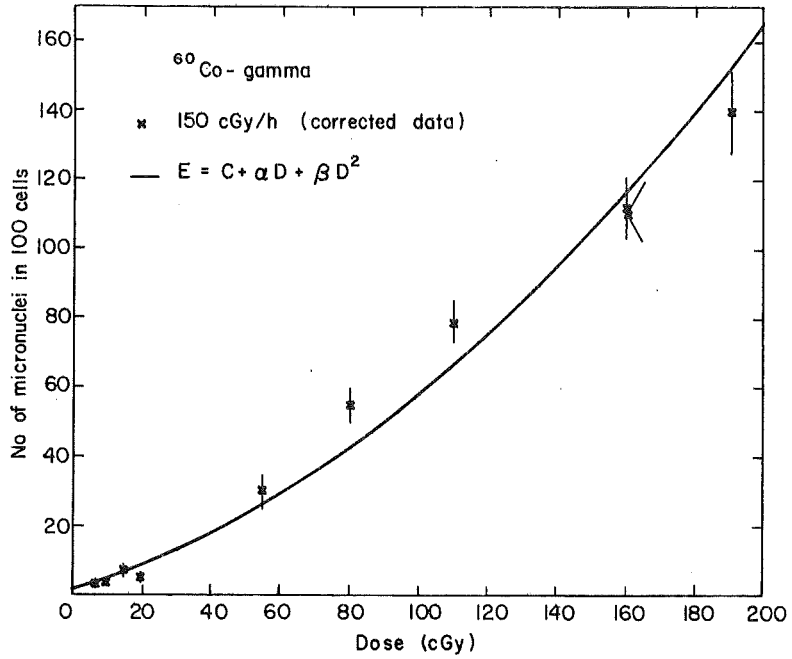

Figure 46: The mean number of micronuclei as function of γ-ray dose for the dose rate of 150 cGy/h.

for the 150 cGy/h curve (fig.49). The values of the coefficients for the 500cGy/h irradiation are: $C=0.15\pm0.02$; $(\beta=5.7\pm0.2)10^{-4}cGy^{-2}$; and for the 150 cGy/h irradiation they are: $C=0.15\pm0.02$; $\beta=(4.7\pm0.2)10^{-4}cGy^{-2}$. Apart from the obviously considerably worse χ^2/f value there will be an underestimation of the effect produced at low doses if only the quadratic term is used to fit the data.

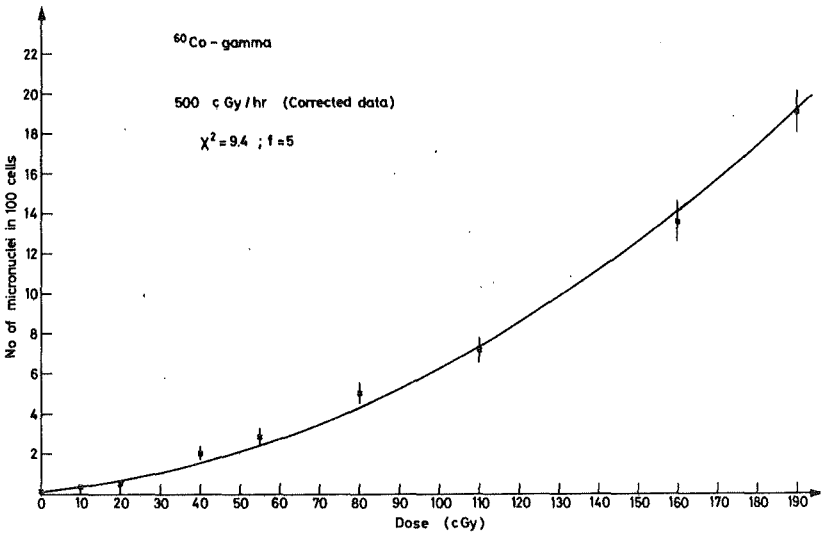

Figure 47: The mean number of micronuclei as function γ-ray dose for a dose rate of 500 cGy/h.

Table 5: The experimental data of the gamma experiments.

Dose-rate (cGy/h)	Dose (cGy)	Mitotic Index (MI)	No of MN/ 100 cells	No of cells with MN/ 100 cells
	0[1]	10.5±0.2	0.13±0.03	0.13±0.02
500	10	11.1±0.4	0.29±0.09	0.26±0.09
	20	11.1±0.2	0.47±0.10	0.45±0.10
	40	10.8±0.5	2.26±0.23	2.10±0.22
	55	9.6±0.3	2.4 ±0.3	2.4 ±0.3
	80	9.2±0.4	4.1 ±0.4	4.0 ±0.4
	110	8.9±0.4	5.7 ±0.4	5.5 ±0.4
	160	10.2±0.5	12.4 ±0.7	11.4 ±0.6
	190	8.1±0.3	13.8 ±0.4	12.0 ±0.4
150	7	9.0±0.5	0.26±0.13	0.23±0.09
	10	9.4±0.5	0.34±0.11	0.32±0.10
	15	9.5±0.5	0.69±0.18	0.66±0.16
	20	11.7±0.3	0.53±0.14	0.48±0.11
	55	10.1±0.4	3.1 ±0.5	3.1 ±0.5
	80	9.4±0.4	4.6 ±0.4	4.3 ±0.4
	110	9.1±0.4	7.5 ±0.4	7.2 ±0.4
	160	11.5±0.6	11.5 ±0.7	10.5 ±0.6
	160	9.2±0.5	10.4 ±0.6	9.4 ±0.5
	190	8.8±0.5	12.7 ±0.6	11.3 ±0.5

1) Meanvalue of all control values.

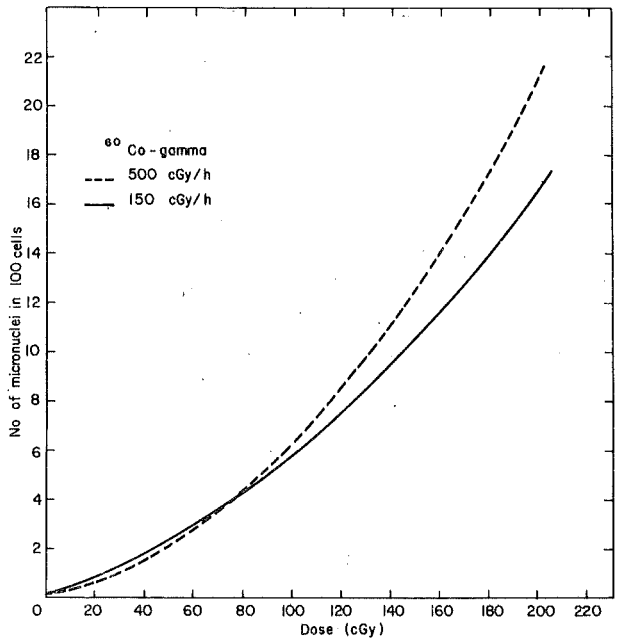

Figure 48: The fitted curves of the two dose-rates of 500 cGy/h and 150 cGy/h plotted together for comparison.

1.3.2 10 cGy/h experiment

In order to ascertain the shape of the dose effect curve at low doses and low LET radiation, doses at an even lower dose rate of 10 cGy/h were given. For high doses it is known that reducing the dose rate results in a reduced effect because the cells will have more time between hits to repair the damage (see also above results). In figure (50) the experimental data for all 3 dose rates up to doses of 20 cGy are given [90,91,92]. All these data points have then been fitted to a linear equation : $E = C + \alpha D$, which gave the following coefficients: $C=0.13\pm0.02$; $\alpha=(1.9\pm0.3)10^{-2}cGy^{-2}$. The χ^2/f value was found to be 0.3 . A linear fit to the experimental data excluding the control value has also been made. The resulting intercept for the fit without controls was 0.11, which is in good agreement with the experimental value of 0.13±0.03. Assuming continuity of the curve, this suggests a linear dose effect relation down to zero dose and thus the absence of a threshold. In Table 6 the experimental data of

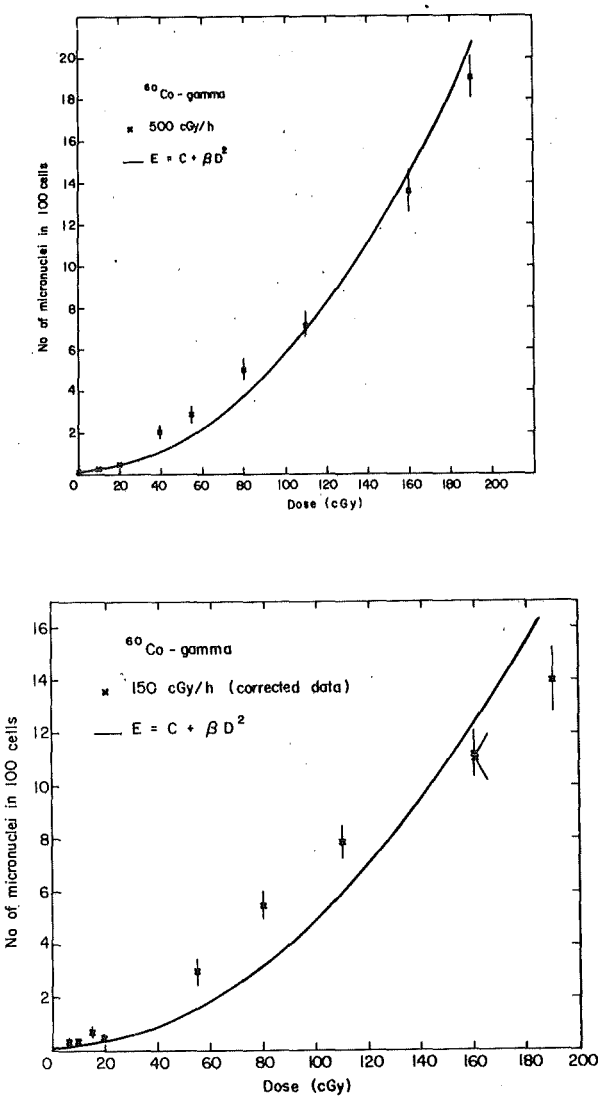

Figure 49: The 500 cGy/h and 150 cGy/h experimental data. after γ-radiation fitted using only the quadratic term.

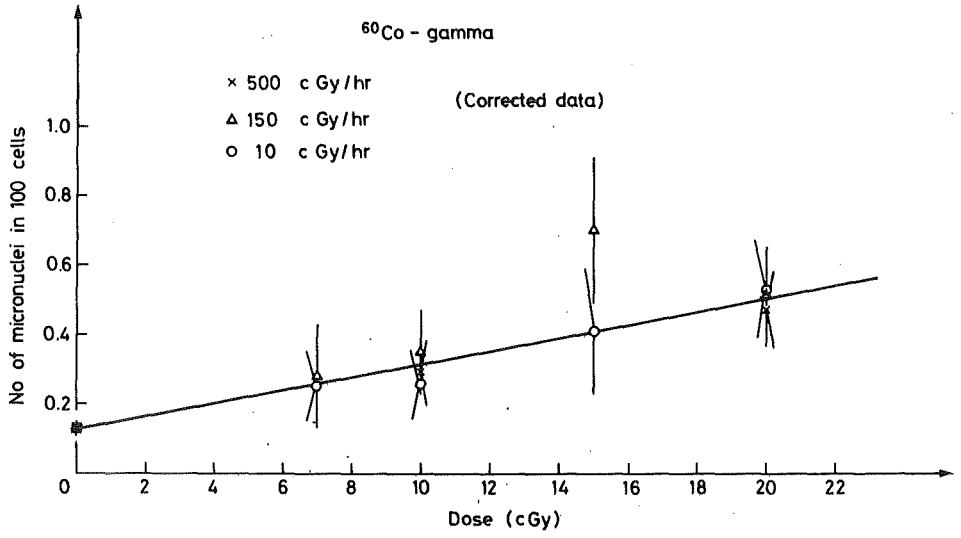

Figure 50: A linear fit to all 3 dose-rate data after γ-radiation.

the low dose rate experiment are listed.

Table 6: Data of the 10 cGy/h gamma-ray experiment.

Dose (cGy)	Mitotic Index (MI)	No of MN/ 100 cells	No of cells with MN/ 100 cells
7	10.2±0.5	0.26±0.10	0.25±0.09
10	10.4±0.5	0.28±0.10	0.26±0.09
15	10.3±0.5	0.43±0.18	0.38±0.10
20	10.5±0.5	0.57±0.13	0.52±0.12

1.3.3 Combining data of different dose rates

Because the data seemed to indicate that there was no obvious dose rate effect below 20 cGy, all the low dose data have been combined and added to the 500 cGy/h as well as to the 150 cGy/h data points, to emphasize the low dose region. The 500 cGy/h and the 150 cGy/h curves were then refitted using both equations, namely :$E = C + \beta D^2$ and $E = C + \alpha D + \beta D^2$. In the case of the linear + quadratic dose effect curve the low dose data were better fitted while the high dose data fit changed very little. The fit became worse when only the quadratic term was used. The following table (Table 7) gives the coefficients and the χ^2/f values obtained for the refitted data.

1.4 π^- plateau and π^- peak

The pion experiment was one of the first experiments carried out for this thesis. At that time the subject of main interest was the effects of fractionation. This is the reason why only two single doses were given, namely 80 and 160 cGy in the plateau region. The other doses were divided into 2 x 80 cGy given between 1 and 24 hours apart. In the peak region also only two doses were given, namely 40 and 80 cGy; the other doses were divided into two times 40 cGy given

Table 7: Coefficients obtained for the combined dose-rates at low doses.

$E = C + \alpha D + \beta D^2$

500cGy/h: $C = 0.12 \pm 0.02$
$\alpha = (1.6 \pm 0.3) * 10^{-2}$ cGy^{-1}
$\beta = (4.5 \pm 0.3) * 10^{-4}$ cGy^{-2}
$\chi^2/f = 1.0$

150cGy/h: $C = 0.12 \pm 0.02$
$\alpha = (1.9 \pm 0.3) * 10^{-2}$ cGy^{-1}
$\beta = (3.4 \pm 0.3) * 10^{-4}$ cGy^{-2}
$\chi^2/f = 2.4$

$E = C + \beta D^2$

500cGy/h: $C = 0.16 \pm 0.02$
$\beta = (5.7 \pm 0.2) * 10^{-4}$ cGy^{-2}
$\chi^2/f = 2.5$

150cGy/h: $C = 0.17 \pm 0.02$
$\beta = (4.8 \pm 0.2) * 10^{-4}$ cGy^{-2}
$\chi^2/f = 4.4$

between 1 and 24 hours apart. In parallel with the irradiations for the micronuclei analysis a 10 day growth experiment was made applying the same doses and fractionation scheme [34]. Unfortunately, it was not possible to add a few more single dose points to the two selected, because this was the last experiment before the shut down of the beam line used. Even though we have not been able to repeat those data or add a few more points the results are still worth presenting. In the following table (Table 8) the experimental data values are given together with the coefficients found for a straight line fit, which was in this case the only possible fit to be made. The ratio of dose needed in the plateau region as compared to the dose needed in the peak region to produce the same effect was found to be 1.7. The same value has been found for the 10 day growth of Vicia faba [23] and for V79 cells in culture [89].

Table 8: The experimental data of the negative pion experiment.

π^--PLATEAU

Dose (cGy)	Mitotic Index (MI)	No of MN/ 100 cells	No of cells with MN/ 100 cells
0	11.6±0.5	0.18±0.05	0.17±0.04
80	8.8±0.5	9.6±0.5	8.7±0.5
160	7.9±0.4	15.8±0.7	14.0±0.6

$E = C + \alpha D$
$C = 0.13 \pm 0.05$
$\alpha = 0.15 \pm 0.01$

π^--PEAK

Dose (cGy)	Mitotic Index (MI)	No of MN/ 100 cells	No of cells with MN/ 100 cells
40	9.7±0.5	9.1±0.5	8.3±0.4
80	9.0±0.4	15.3±0.6	13.5±0.5

$E = C + \alpha D$
$C = 0.13 \pm 0.05$
$\alpha = 0.25 \pm 0.01$

2. Split dose experiments

Fractionating or splitting a dose means that a dose is divided into two equal parts and the second dose is given a certain time interval after the first dose. In this way cells are given time to repair the still repairable damage produced by the first irradiation. One would expect a reduced effect after such a treatment, as compared to single dose exposure [31]. It has just been mentioned that fractionation experiments were also carried out using the 10 day growth as a test. The radiations used in this case were pion, high energy neutrons and ^{60}Co-γ- radiation [34,35]. The results indicated that already after about 1 hour most of the repair has taken place. This

reason, together with the fact that prolonging the time interval beyond 1 hour produces cell kinetic problems due to the G2-blockage, convinced us that the 1 hour split dose was the obvious time period to use when discussing repair.

2.1 SC-neutrons

In the case of the high energy neutrons a dose of 40 cGy has been split into two half doses given 1 hour apart. The results in comparison to the corresponding single dose result obtained during the same experiment is given in Table 9.

Table 9: Experimental data of the neutron split dose experiment.

Dose (cGy)	Mitotic Index (MI)	No of MN/ 100 cells	No of cells with MN/ 100 cells
40	8.3±0.4	13.1±0.6	11.2±0.5
(20+20) (1h split)	8.0±0.4	15.6±0.6	13.3±0.5

From the data it is obvious that no recovery has taken place.

2.2 ^{60}Co-γ-rays

A split dose experiment has only been carried out for the high dose rate (500 cGy/h).Total doses of 190,160,110 and 40 cGy have been split in half and were administered one hour apart. As can be seen from figure (51) the expected recovery at high dose has taken place while it is completely absent at the low dose [92].
The coefficients used for the fit were: $C=0.13\pm0.03$; $\alpha=(3.8\pm0.8)10^{-2}cGy^{-1}$; $\beta=9.1\pm6.2\ 10^{-4}$. In Table 10 the experimental data are given.

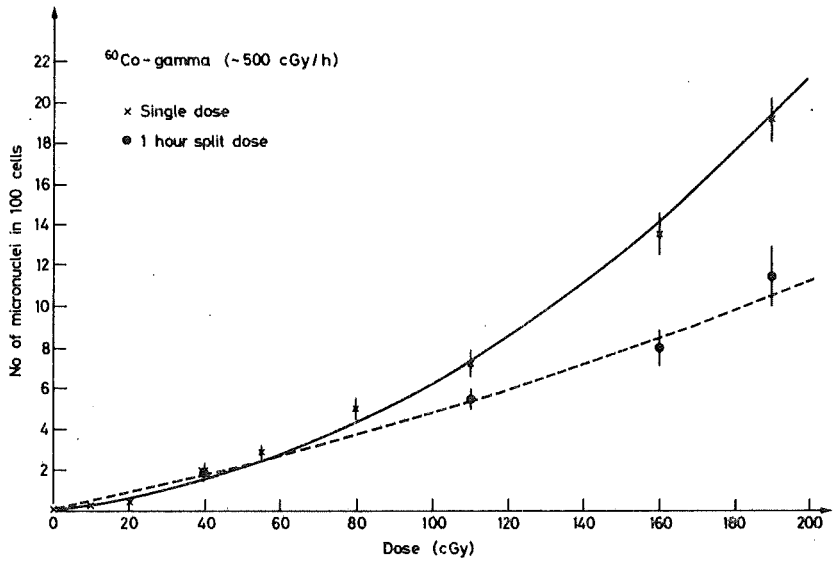

Figure 51: The experimental results of the split doses in comparison to the single dose results (both at a dose-rate of 500 cGy/h).

Table 10: Experimental data of the gamma-ray split dose experiment.

Dose (cGy)	Mitotic Index (MI)	No of MN/ 100 cells	No of cells with MN/ 100 cells
40	10.8±0.5	2.26±0.23	2.10±0.22
(20+20)	10.0±0.4	1.86±0.23	1.77±0.22
110	8.9±0.4	5.7±0.4	5.5±0.4
(55+55)	9.8±0.4	4.6±0.4	4.4±0.4
160	10.2±0.5	12.4±0.7	11.4±0.6
(80+80)	9.8±0.4	6.7±0.5	6.3±0.4
190	8.1±0.3	13.8±0.4	12.0±0.4
(95+95)	9.1±0.4	9.3±0.5	8.5±0.5

2.3 π^--plateau and π^--peak

In the plateau region a total dose of 160 cGy and in the peak region a dose of 80 cGy has been divided into two equal halves given 1 hour apart. Only a small amount of recovery is observed in both cases. The experimental data of the pion irradiation are shown in figure (52).

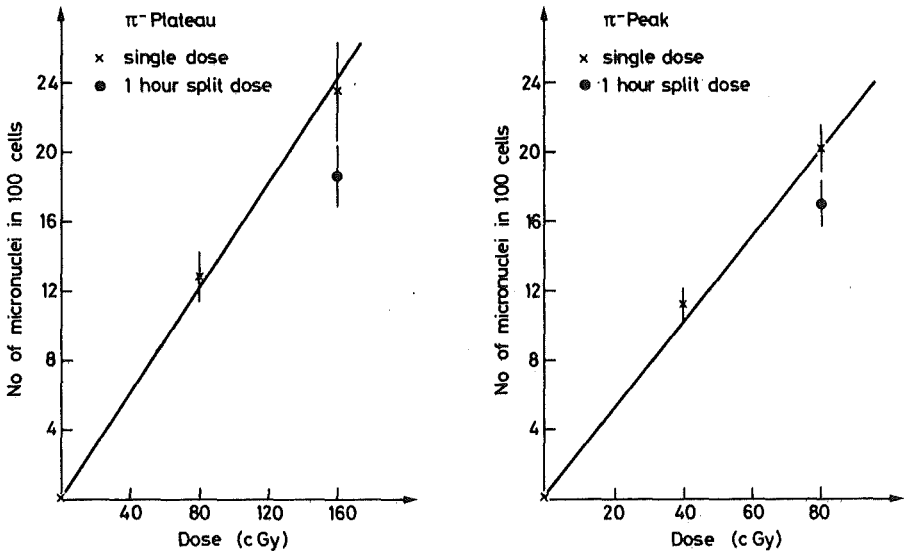

Figure 52: The results of the single dose and split dose pion experiment a) plateau and b) peak.

The damage produced by the pions in the peak region is about a factor of 2 higher than that produced by the pions from the plateau region.

3. Oxygen effect

It is a well known fact that the oxygen effect observed after irradiations with high LET particles is smaller than the one exhibited using low LET radiation. However, there are also indications of a reduction of the oxygen effect at low doses in the case of low LET radiation [93].

To be sure that the hypoxic condition by itself does not produce micronuclei in the bean root meristem, 3 control groups were kept 1,2,3 and 4 hours under anoxic conditions, whereas 3 hours has been the maximum time period for the irradiated beans to stay in anoxia (fig.53).

As can be clearly seen, no additional micronuclei are produced and the anoxic control group is identical to the oxic control group. The experiment under hypoxic conditions was carried out giving a wide range of doses, 7 - 600 cGy of ^{60}Co-γ-rays (500 cGy/h). The percentage mitotic index as function of dose is shown in figure 54.

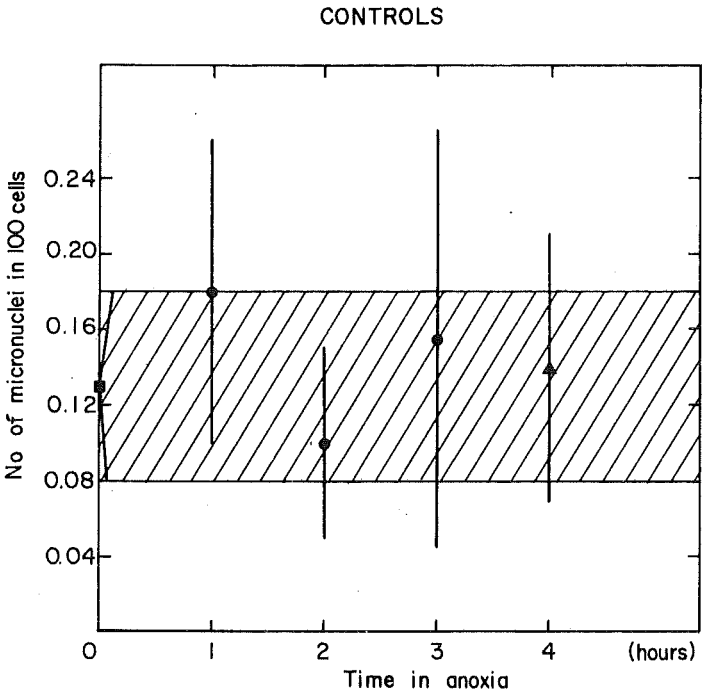

Figure 53: The number of micronuclei in the anoxic control groups as a function of time in anoxia.

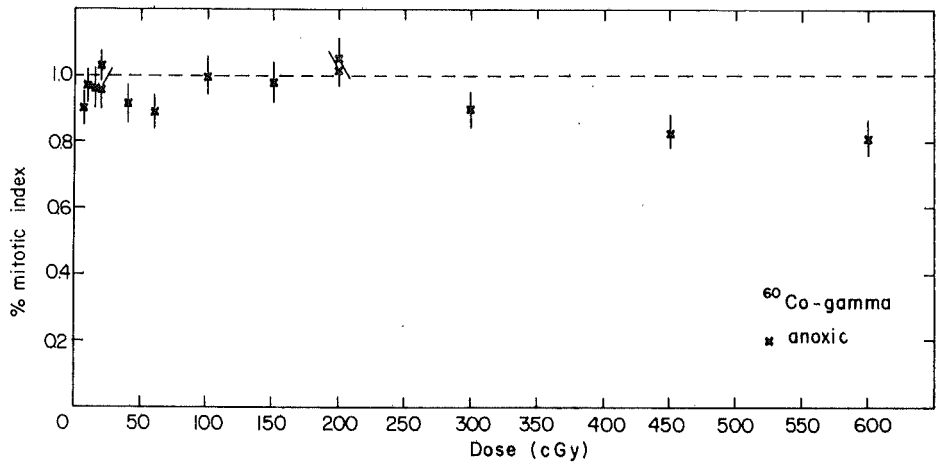

Figure 54: The percentage mitotic index of the anoxic experiment as a function of dose.

The corrected data are plotted together with the experimental results of the aerated experiment in figure (55). It can be seen that at high doses a strong oxygen effect is observed. In the lower dose region, however, no difference is visible. This fact is illustrated even more clearly in figure (56), where all the low dose experimental data of the three different dose rates of the aerated experiment were combined with the results from the beans irradiated in hypoxia.

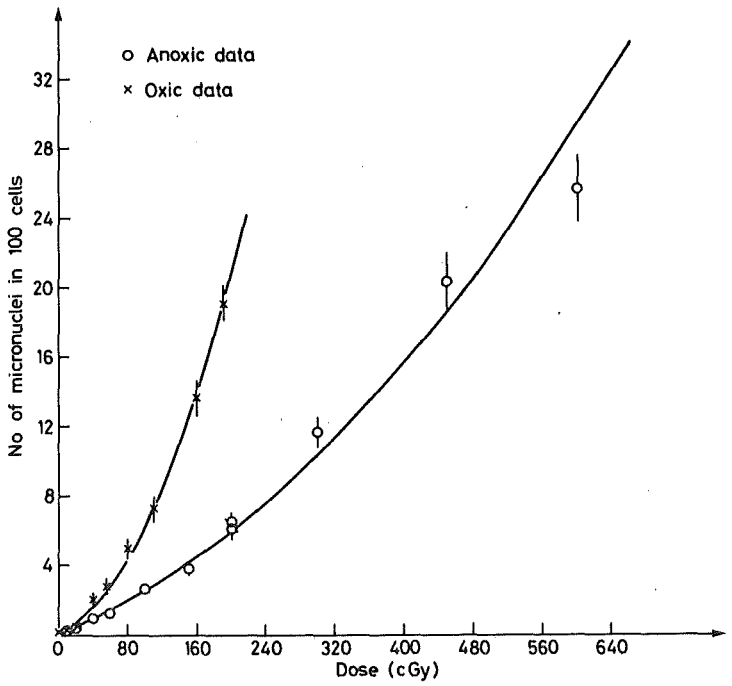

Figure 55: The oxic and anoxic data are both fitted to the linear+quadratic equation.

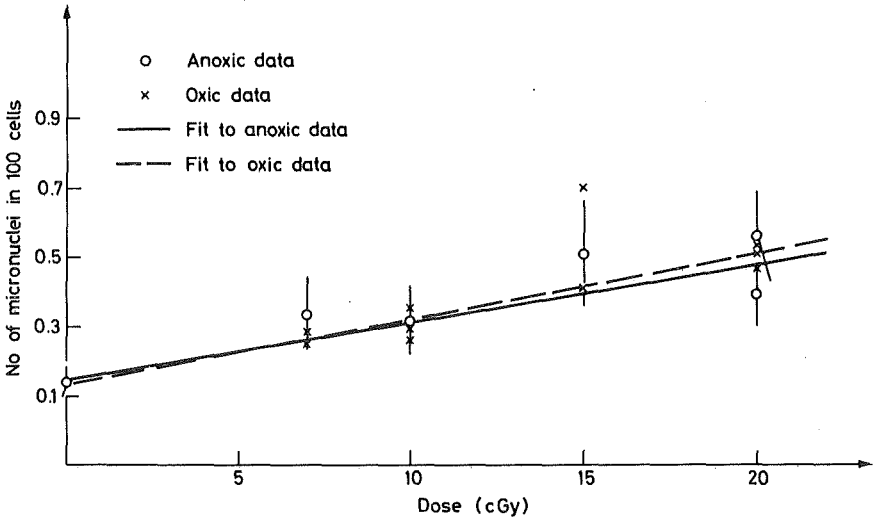

Figure 56: The anoxic low dose data (with error bars) are plotted together with the oxic low dose data (without error bars). Both data sets were fitted independently to a linear equation.

No difference is observable and the OER value is therefore one for doses up to 20 cGy. In Table 11 the anoxic experimental data are given. They have been fitted to a linear+quadratic equation with the coefficients of: $C = 0.13 \pm 0.03$; $\alpha = (1.9 \pm 0.2)10^{-2} cGy^{-1}$; $\beta = (4.9 \pm 0.6)10^{-5} cGy^{-2}$ and with a χ^2/f of 1.35.

Table 11: The experimental data of the two anoxic experiments.

Dose (cGy)	Mitotic Index (MI)	No of MN/ 100 cells	No of cells with MN/ 100 cells
$0^{1)}$	10.3±0.3	0.15±0.05	0.13±0.04
$0^{2)}$	10.9±0.4	0.14±0.07	0.13±0.06
$7^{2)}$	9.8±0.4	0.31±0.09	0.28±0.08
$10^{2)}$	10.6±0.4	0.31±0.10	0.29±0.08
$15^{2)}$	10.5±0.5	0.49±0.14	0.44±0.12
$20^{2)}$	11.2±0.4	0.40±0.09	0.40±0.09
$20^{1)}$	9.9±0.5	0.54±0.12	0.51±0.11
$40^{2)}$	10.0±0.5	0.89±0.17	0.81±0.16
$60^{1)}$	9.2±0.4	1.05±0.15	1.04±0.14
$100^{2)}$	10.9±0.5	2.6±0.3	2.5±0.3
$150^{2)}$	10.7±0.5	3.8±0.3	3.5±0.3
$200^{2)}$	11.1±0.4	6.3±0.4	5.8±0.4
$200^{1)}$	10.8±0.5	6.8±0.4	6.4±0.4
$300^{2)}$	9.8±0.4	10.5±0.5	9.4±0.4
$450^{2)}$	9.0±0.5	16.9±0.8	14.4±0.6
$600^{2)}$	8.9±0.5	20.8±0.9	17.5±0.7

The indices 1) and 2) refer to two separate experiments.

4. RBE-values

The RBE (Relative Biological Effectiveness) value is used to compare the efficiency of different types of radiation with that of ^{60}Co-gamma rays. It is defined as being the ratio of the two doses (D(γ)/D(radiation)) which are needed to produce the same effect. If the curve which is compared to the gamma ray curve is for example represented by a straight line, the RBE value will vary with dose. However, if the gamma ray curve displays a linear initial slope the RBE will assume a constant value at low doses.

In figure (57) the two RBE-curves found for the SC- and the ^{252}Cf-neutrons when compared to the 500 cGy/h γ-ray data are presented. The maximum RBE-value of the high energy neutrons in the very low dose region was calculated to be : 31.0 ± 6.4 and for the

^{252}Cf-neutrons to be: 76.8 ± 16.8.

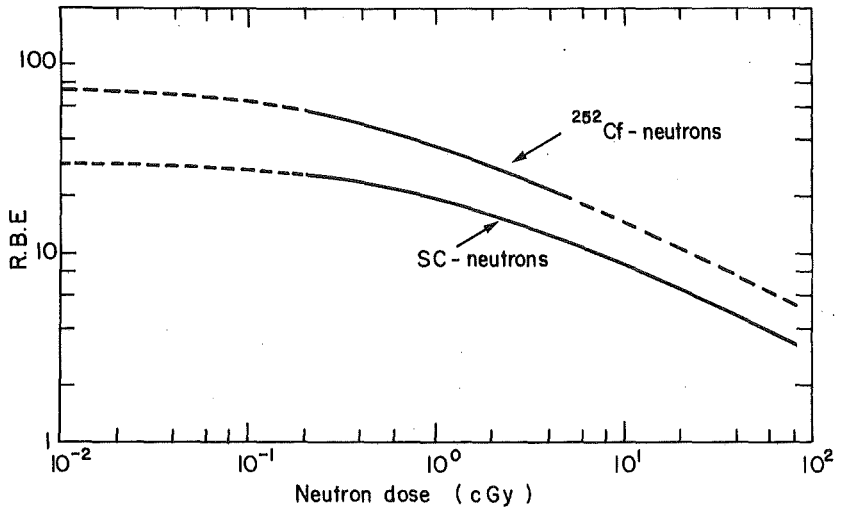

Figure 57: The two RBE-curves calculated from the fitted curves of the SC- and ^{252}Cf-neutrons in comparison to the ^{60}Co-gamma curve (500 cGy/h). The dotted lines represent areas were no experimental values were measured.

In the following table (Table 12) all the RBE values found for the different radiation qualities in comparison to different γ-ray data sets are given.

Table 12: The maximum RBE values for the different radiation qualities.

Dose-rate (cGy/h)	SC-neutrons	^{252}Cf-neutrons
500	26.5±3.1	66.5±9.2
500[1]	31.0±6.4	76.8±16.8
150	15.0±1.2	37.6±4.1
150[1]	24.6±4.4	61.7±11.7
10,150,500[2]	25.4±4.4	63.7±12.0

1: Below 20 cGy all dose-rates are combined
2: RBE was calculated from the linear fit made to all dose-rates below 20 cGy.

The RBE values found at an effect level of 190 micronuclei/100 cells which corresponds to a gamma-ray dose of 190 cGy was found to

cells which corresponds to a gamma-ray dose of 190 cGy was found to be 4.7±0.4 for the SC-neutrons and 11.8±1.3 for the ^{252}Cf-neutrons. The RBE-values found for the negative pion plateau region was 1.3 and 1.8 for the 160 and 80 cGy dose respectively. In the case of the stopped pions the RBE varied between 2.45 and 3.3 for the 80 and 40 cGy irradiation. It should be mentioned that the dose values given here correspond to the total dose and no correction for the gamma contamination has been made.

CHAPTER VII

DISCUSSION

Chromosome damage leading to acentric or dicentric aberrations is generally considered as being too severe an injury for a cell to survive. Many authors have reported correlations between DNA double strand breaks and reduction in survival rate [77,94,95], strengthening this assumption. The same correlation should exist for micronuclei because they are formed from acentric fragments. The 10 day-growth curve can be considered as a type of survival curve because an increase in cell killing will be proportional to a reduction in growth of the root. Therefore, the percentage 10 day growth data for high energy neutron doses of:25,37,56,60,74,90 and 92 cGy were plotted against the number of cells with micronuclei observed for the corresponding doses (fig.58).

A very good correlation between these two effects is obvious. This agrees with the data reported by Grote et al.[96,97] who have found direct evidence for a relation between micronuclei formation and slow-growth or stop-growth of colonies in cell in culture systems. The authors were able to observe single cells for several mitoses after X-ray irradiation and concluded that micronuclei formation finally leads to the death of the cell.

A very good linear correlation was also obtained when the number of cells with micronuclei was plotted against the number of micronuclei for two radiation qualities, namely the high energy neutron- and

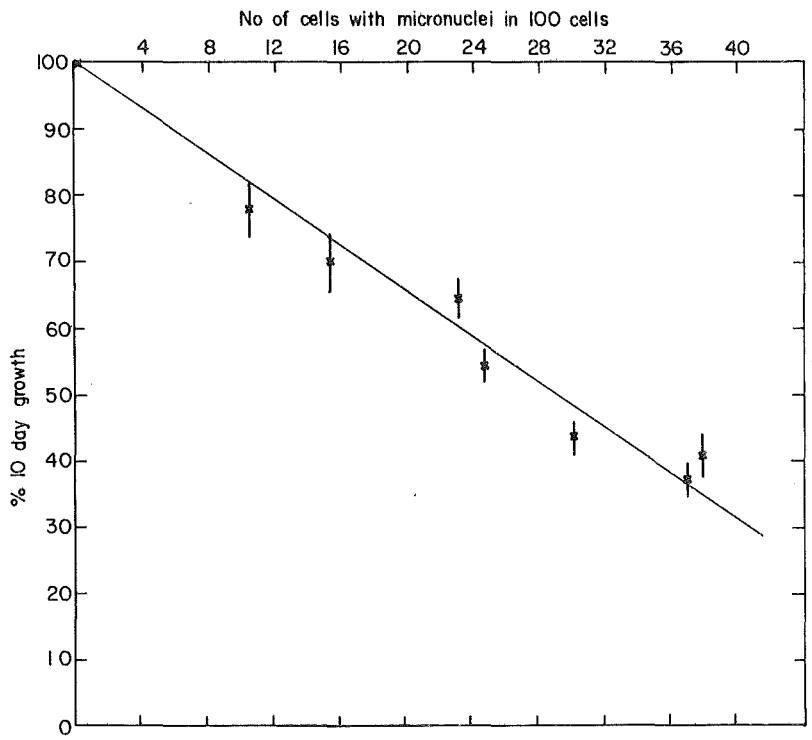

Figure 58: The percentage 10 day-growth as a function of number of cells with micronuclei.

the 500 cGy/h γ-ray-radiation (fig.59). This proportionality indicates that the average multiplicity of micronuclei is a constant.

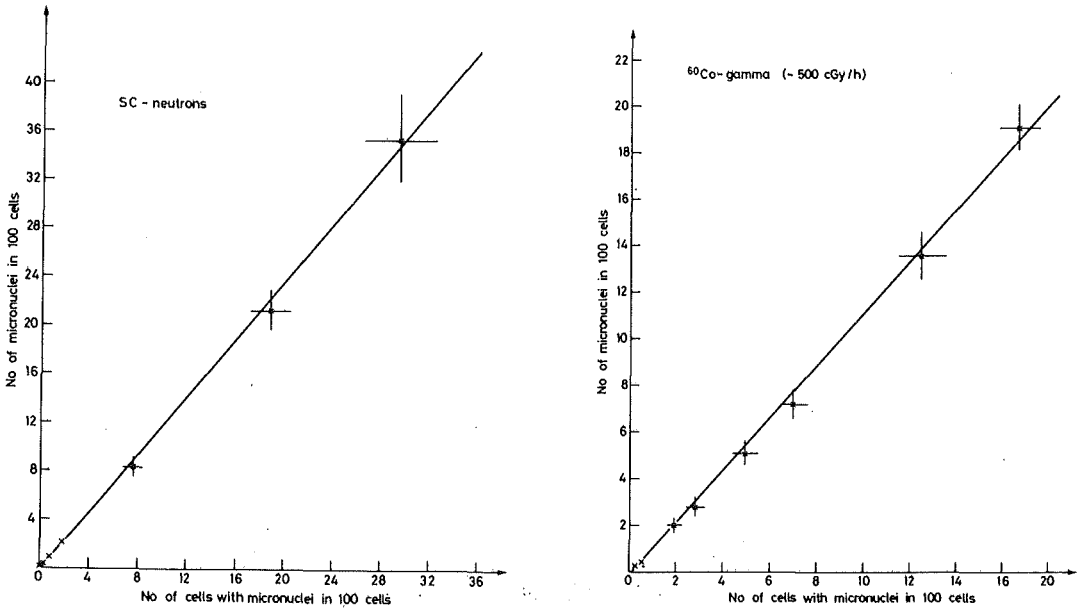

Figure 59: The number of cells with micronuclei is plotted against the number of micronuclei.

These correlations allow an extension of the discussion of the dose

effect curves from mere chromosome aberration incidence to cell killing.

An important result of the analysis of the single dose experiments has been the clear evidence of a linear dose effect relationship at low doses for all radiation qualities used. In the case of high LET particles this linear dependence continues also in the high dose region while for low LET radiation the quadratic dependence becomes dominant. In the theory of dual radiation action it is postulated that ionizing radiation produces so called "sublesions" in the cells of higher organisms. These sublesions combine in pairs to produce the lesions which are responsible for the various biological effects observed, eg. chromosome aberrations. In the case of high LET radiation these sublesions can be produced by one single particle because of its high ionization density. In the case of low LET radiation, which is also called sparsely ionizing radiation, more than one particle is needed to produce the final lesion. However, the LET is a function of the velocity of the particle traversing a medium (see Bethe-Bloch formula in the dosimetry section) and the energy loss per unit path-length increases with decreasing energy. In the following figure(60) the distribution of dose in z (the specific energy) for single events in a spherical tissue region of 1µm for ^{60}Co-gamma, 14.7 MeV and 3.7 MeV neutrons is plotted.

The ^{60}Co-gamma distribution extends far into the region of the 14.7 MeV neutrons and reaches even into the 3.7 MeV neutron distribution. If regions below 1µm are considered the ionization density produced can be still higher. For example an electron with a kinetic energy of 100 eV will lose all its energy within a region of 20 10^{-10}m which is about the diameter of a DNA molecule [98]. This very localized energy deposition of 100 eV corresponds to a LET value of about 50 keV/µm which is now even comparable to the LET of a very low energy

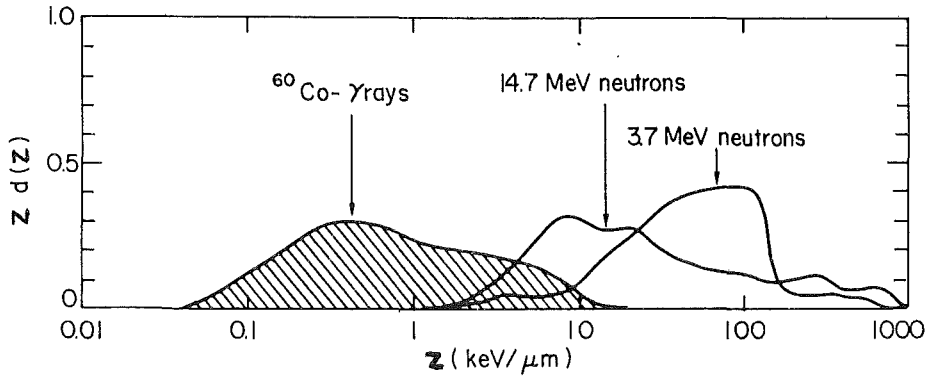

Figure 60: The distribution of dose in z.

neutron, and therefore belongs clearly to the group of high LET radiation (>10 keV/μ). This very small but certainly existing high LET component in the gamma radiation is the cause of the linear dependence between dose and effect at low doses. The probability that two independent particles would interact at low doses to produce an effect is negligible and therefore only the single particle interaction is important in this dose region.

Clear evidence of a linear dose-effect relationship at low doses was, to my knowledge, first reported by Sparrow and Underbrink [99], who studied the mutation incidence in Tradescantia after X-ray irradiation. The more recently published data from Furcinitti and Todd [100] also shows a linear dependence in a dose region between 20 and 80 cGy for human kidney cells in culture, after irradiation to X-rays. A linear-quadratic relationship was also reported by Lloyd et al.[101] for chromosome aberrations in human lymphocytes after irradiation to γ- and x-rays. By calculating $\lambda=\alpha/\beta$, where α and β are the coefficients from the linear+quadratic equation, one obtains the dose value where the linear and the quadratic term contribute equally to the effect. In the case of the 500 cGy/h curve (see table 7) λ is found to be equal to 34.5 ± 7.3 cGy, while for the 150 cGy/h λ = 57.5 ± 11.0 cGy. The dose region where the linear part is domi-

nant was, in the case of the mutation studies, below 18 cGy, while in the case of human kidney cells in culture this value was much higher (above 80 cGy). The α/β value of the human chromosome aberration studies from Lloyd et al. was 31 for dicentrics, 59 for acentrics and 40 cGy for the total amount of aberrations. These values agree well with the ones found here for micronuclei induction, which shows the comparability of the results found for Vicia faba with human data.

The existence of a high LET component in the gamma experiment can be an explanation for the non-existence of dose-rate, fractionation and oxygen-effect. The lack of recovery between doses and for reduced dose-rates in the linear part is similar to the effect observed after neutron and negative pion irradiation. Using as a test the 10 day growth of Vicia faba, less recovery was found for negative pions in the peak region when compared with the recovery in the plateau region. This results in an increased gain factor between the plateau and peak region and is of great importance for radiotherapy [34,102,103]. The same result has been obtained using micronuclei induction (figs 47a+b).

In the case of the fractionation experiment using high energy neutrons, no recovery at all was found. Again, this agrees with the results found from a 10 day growth experiment carried out using the same beam [35], where doses between 20 and 90 cGy were divided into two and 3 equal fractions each given 24 hours apart. No recovery was observed at low doses while at high doses an enhancement in effect was actually found. A similar result has been obtained by Vogel et.al.[104] studying mammary tumor induction in rats. These results can be partly explained with the Elkind theory of recovery which says that the amount of recovery of which a system is capable depends on the size of its survival shoulder. From a linear dose effect curve

which is equivalent to an exponential survival curve (see Table 1.) no recovery between doses, or at a lower dose rate, should be expected.

Another similarity between γ-rays at low doses and high LET radiation is that no oxygen effect is observed up to a dose of about 20cGy(eg. OER=1). Recently Underbrink and Wolch [93] reported that in the case of mutations in Tradescantia stamen hairs, the OER seemed to approach unity at low doses. In the case of cell killing this effect has not yet been studied. An explanation for so drastic a reduction in oxygen effect might be that the damage produced by the high LET component of the gamma radiation will be mostly unrepairable DNA double strand breaks. Therefore, the micronuclei production will not be altered by the presence or absence of oxygen in the low dose region. Above 20 cGy the quadratic component becomes more and more important, and from then on the anoxic curve departs from the oxic curve. For the anoxic curve the α/β-value was found to be: λ=385.0±59.0 cGy. It is obvious that in the absence of oxygen the linear component is dominant much longer.

Linearity at low doses should actually reduce the problems of risk estimates for different radiation qualities because it implies that the RBE value reaches a constant value (equal to the ratio of the slopes of the two lines) in the dose region of interest for radiation protection. In figure (61) a comparison is made between the results of other experiments with the RBE values found here for the high energy neutrons and ^{252}Cf-neutrons, which were in the low dose region approaching values of 31.0±6.4 and 76.8±16.8 respectively.

There is a very good relationship between data of RBE values measured for mutation, transformation, eye lens opacification and cell killing. An experiment carried out here at CERN using the same high energy neutron beam (SC) to study the eye lens opacification in mice

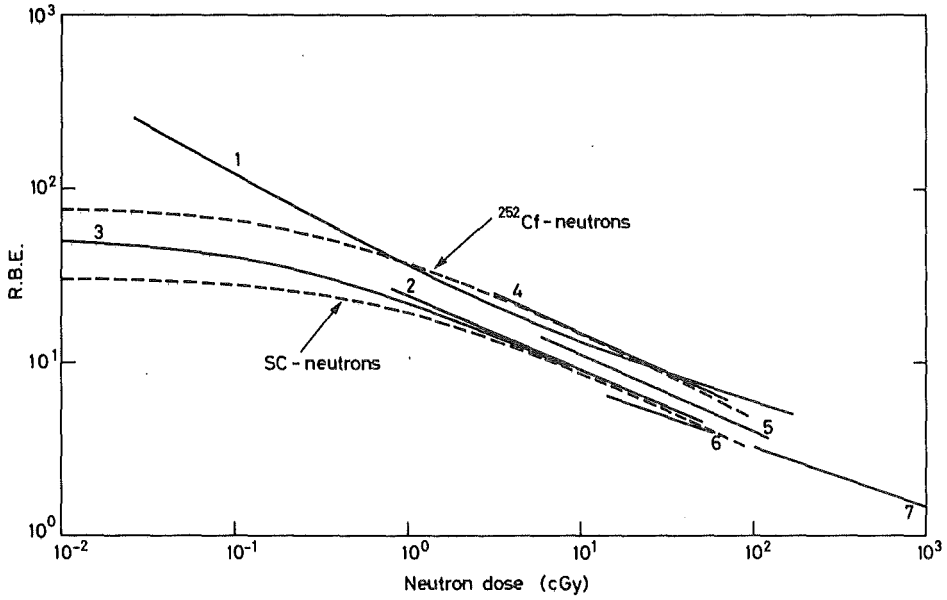

Figure 61: The RBE curves found for micronuclei induction as compared to the RBE curves found for different effects. 1) Opacification of the murine lens [105], 430 keV neutrons. 2) Opacification of the murine lens [105], 1.8 MeV neutrons. 3) Mutations of Tradescantia stamen hairs [99], 430 keV neutrons. 4) Mammary neoplasm in the Sprague-Dawley rat [106], Fission neutrons. 5) Chromosome aberrations in human lymphocytes [107], Fission neutrons. 6) Growth reduction of Vicia faba root [108], 6.0 MeV neutrons. 7) Skin damage (human, rat, mouse, pig) [109], 6.0 MeV neutrons.

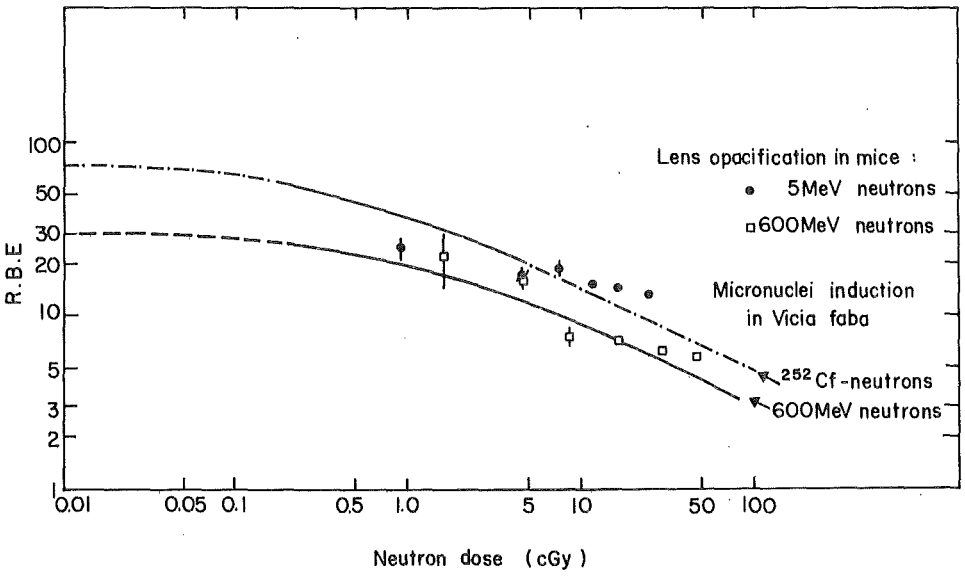

Figure 62: A comparison of the RBE curves found for micronuclei induction with the RBE values found for lens opacification in mice.

resulted in about the same RBE-values [110]. These data, together with data obtained using low energy neutrons (2.35 MeV) are presented

in figure (62). The RBE values found for the high dose data are in close agreement with the values obtained from the 10 day-growth and for survival curves derived from the 10 day-growth [23,22]. The RBE values found for the negative pions in the plateau-region, which varied between 1.3 and 1.8, and the RBE values found for the peak-region, which varied between 2.45 and 3.3, are similar to those reported in literature [23,111,112,113,114,115,116].

The fact that different tests still give about the same RBE values is very important . Furthermore, these values are, at low doses, independent of any dose modifying factors such as oxygen, dose rate, or fractionation.

There are three more points worth stressing. One is the fact that the dose response of a system depends very much on dose, dose-rate and radiation quality used. Radiation very often induces a delay in the cell progression and a lengthening of the cell cycle time, thus changing the time of appearance of the effect being studied. By using only one fixation point this time alteration is not taken into account and one can very easily obtain a wrong result. As has been shown in this work a very strong delay was found with neutrons, while in the case of gamma radiation the mitotic index dropped only to 80% of the control value. A similar bend over of the dose-effect curve at high doses of neutrons was observed by Vulpis et.al. [117] using the same high energy neutron beam and by Molls et. al.[118], suggesting the same qualitative response to this radiation.

The second point to be mentioned is the danger of predicting low dose effects using high dose data alone. The data for micronuclei induction were refitted with the linear + quadratic equation, using only data points above 20 cGy which were already well into the quadratic region. An overestimation by a factor of 1.7 was found for the linear part in the case of the 500 cGy/h curve and a factor of 1.8

for the 150 cGy/h curve.

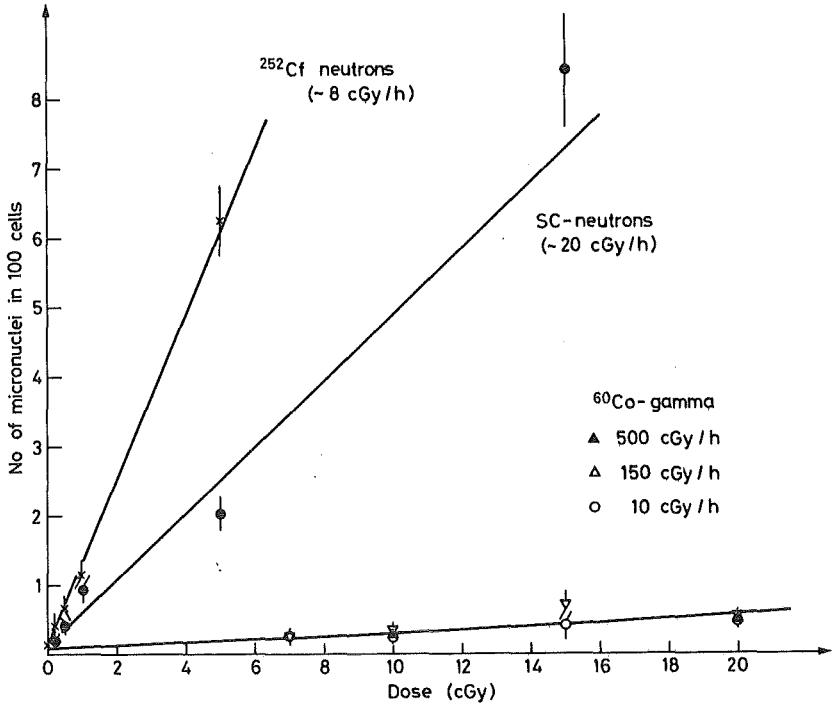

Figure 63: Comparison of effects produced by neutrons and gamma rays in the low dose region.

Finally, even though the effect produced by gamma rays is relatively small it should not be forgotten that the damage produced in the low dose region increases linearly with dose and does not seem to be repairable; this implies no threshold response. The effect produced by neutrons, however, is much more significant and should be taken very seriously. In figure (63) a comparison of the low dose data for both neutron energies and γ-rays are given. This large difference in effect persists even to higher doses as is shown in figure (64). One notes that the low energy neutrons are by far the most damaging radiation of all radiation qualities studied here.

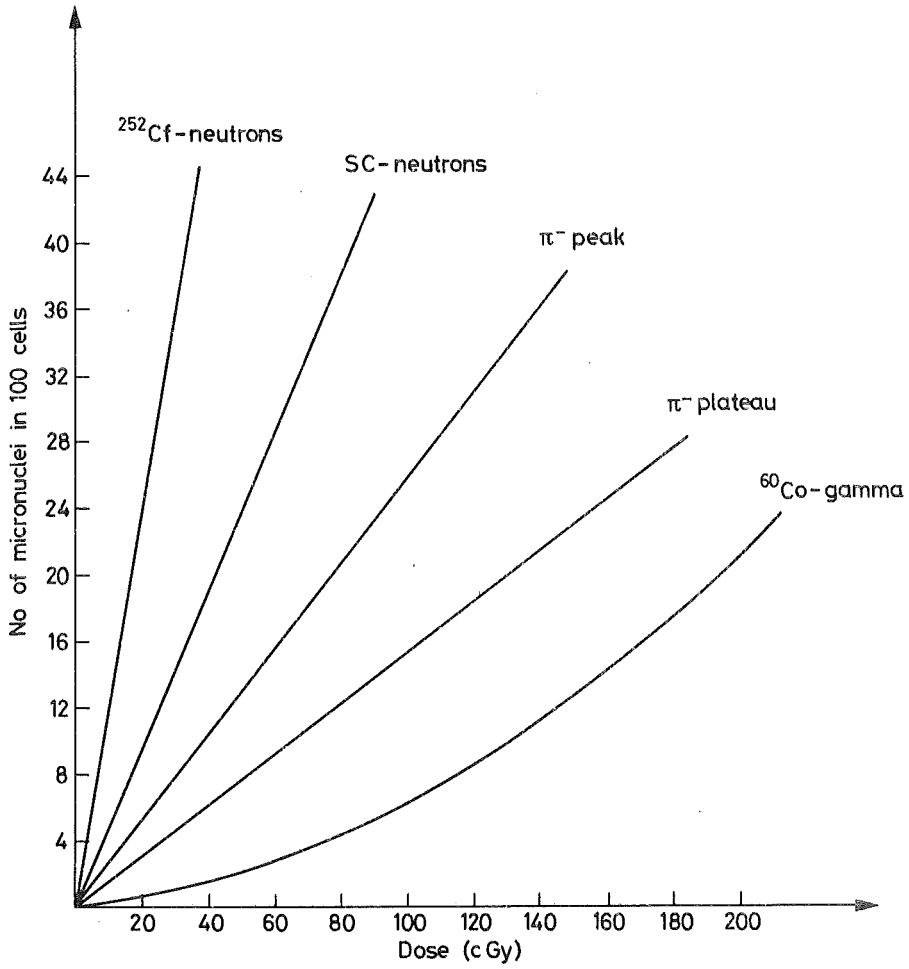

Figure 64: Intercomparison of the effects produced by different radiation qualities.

SUMMARY

The results of this work have shown that in the case of micronuclei induction in Vicia faba the dose-effect curve is much better described by a linear + quadratic than by a purely quadratic equation for low LET radiation.

For the high LET radiation used here (SC-neutrons, ^{252}Cf-neutrons, pions) a linear dose-effect relationship was found.

The necessity of normalizing the experimental data to mitotic index fluctuations has been shown to be very important for establishing dose effect curves.

The linearity observed at low doses for all radiation qualities results in constant RBE values in the dose region of interest for radiation protection.

The linear part of the dose-effect curve for low-LET radiation has been shown to be independent of three major dose modifying factors: oxygen, dose rate and dose fractionation.

In the case of high-LET radiation no or very little repair between doses was found.

These results confirm the predictions of dual radiation theory which is based on microdosimetric findings that so called low-LET radiation also contain a high-LET component.

REFERENCES

1) National Research Council. Washington. Committee on the biological effects of ionizing radiations. The effects on Population of Exposure to Low Levels of Ionizing Radiation : 1980 National Academy Press, Washington, D.C. 1980.

2) High Background Radiation Research Group, China Health survey in high background radiation areas in China. Science, Vol.209, pp.877-880, (1980).

3) Fabrikant,J.I. The BEIR-III report and the health effects of low-level radiation. Lawrence Berkeley Laboratory (LBL-10383), January 1980.

4) Nias,A.H.W., Greene,D., Fox,M., Thomas,R.L. Int. J. Radiat. Biol., Vol.13, pp.449-456, (1967).

5) Dessauer,Fr. Ueber einige Wirkungen von Strahlen. I. Zeitschrift fuer Physik,12, pp 38-47,1922.

6) Blau,M. and Altenburger,K. Ueber einige Wirkungen von Strahlen. II. Zeitschrift fuer Physik,12, pp 315-329,1922.

7) Lea, D.E. Actions of radiations on living cells. Cambridge : University Press, 1946.

8) Timofeeff-Ressovsky,N.W. and Zimmer,K.G. Biophysik I : Das Trefferprinzip in der Biologie. Leipzig : Hirzel, 1947.

9) Tobias,C.A., Blakely,E.A., Ngo,F.Q.H. and Yang,T.C.H. The repair-misrepair model of cell survival. Lawrence Berkeley Laboratory (LBL-9121),June 1980.

10) Leenhouts,H.P., Chadwick,K.H. The crucial role of DNA double-strand breaks in cellular radiobiological effects. Advances in Radiation Biology Vol.7, pp.55-101,1978.

11) Kellerer,A.M. and Rossi,H.H. The theory of dual radiation action. Current Topics in Radiation Research Quarterly,

Vol.8, No.2,(1972).

12) Kellerer,A.M. Micro-distribution of energy deposition and the biological effectiveness of ionising radiations. Sonderdruck aus der Fachzeitschrift "Kerntechnik" 20Jg. 1978 Heft 7 pp.301-311. Verlag Karl Thiemig.

13) Kellerer,A.M. Mikrodosimetrie : Grundlagen einer Theorie der Strahlenqualitaet. Gesellschaft fuer Strahlenforschung M.B.H. Muenchen;GSF-Bericht B146, November 1968.

14) Mottram,J.C. On the action of beta and gamma rays of radium on the cell in different states of nuclear division. Arch.Middlesex Hosp. London, 30, 98-119, (1913).

15) Howard,A., Pelc,S.R. Synthesis of desoxyribonucleic acid in normal and irradiated cells and its relation to chromosome breakage. Symp. on chromosome breakage. Suppl. to Heredity,6, pp 261-273,1952.

16) Thoday,J.M. and Read,J. Nature, London,160,608,1947.

17) Sax,K. The behaviour of X-ray-induced chromosomal aberrations in Allium root tip cells. Genetics,26,418-425,1941.

18) Gray,L.H.,Read,J.,Mottram,J.C. Comparison of the lethal effect of fast neutrons and γ-rays on the growing tips of broad bean roots. Nature, Vol.144, pp.478-479, (1939).

19) Gray,L.H.,Scholes,M.E. The effect of ionizing radiations on the broad bean root. Part VIII : Growth rate studies and histological analysis. Brit. J. Radiol. 24, 82-92, 176-180, 228-236, 285-294, 348-354, (1951).

20) Read,J. Radiation biology of Vicia faba in relation to the general problem. Blackwell scientific publications, Oxford BS 1959.

21) Baarli,J., Bianchi,M. Observed variations of RBE values in the stopping region of a 95 MeV negative pion beam. Int. J. of

Rad. Biol., Vol 22, No2, pp 183-186, 1972.

22) Laurent,J.M. Effet sur la racine principale de Vicia faba de l'exposition aux rayons gamma du ^{60}Co aux protons de 600 MeV et aux neutron de 14 Mev et de 400 MeV. CERN, 74-25, 1974.

23) Hill,C.K. and Baarli,J. RBE and OER values from 10-day growth inhibition of Vicia faba roots exposed to high-energy neutrons and pion beams. CERN 79-05 Health and Safety Division, 20 June 1979.

24) Kihlman,B.A. Root tips of Vicia faba for the study of the induction of chromosomal aberrations. Mutation Research, 31, 401-412,(1975).

25) Clowes,F,A.L. Apical meristems of roots. Biol.Rev., Vol.34, pp.501-529, (1959).

26) Scott,D. and Evans,H.J. X-ray induced chromosomal aberrations in Vicia faba: Changes in response during the cell cycle. Mutation Research,4, pp 579-599,1967.

27) Evans,H.J.,Neary,G.J. and Williams,F.S. The relative biological efficiency of single doses of fast neutrons and gamma rays on Vicia faba roots and the effect of oxygen. Part II : Chromosome damage: the production of micronuclei. Int. J. Rad. Biol., Vol.3, pp.216-229, (1959).

28) Matter,B.,Schmid,W. Trenimon-induced chromosome damage in bone marrow cells of six mammalien species, evaluated by the micronucleus test. Mutation Research, Vol.12, pp.417-425, (1971).

29) Lederbur von,M. and Schmid,W. The micronucleus test methodological aspects. Mutation Research, Vol.19, pp.109-117, (1973).

30) Heddle,J.A. A rapid in vivo test for chromosomal damage.

Mutation Research, Vol.18, pp.187-190, (1973).

31) Elkind,M.M. and Sutton,H. Radiation response of mammalian cells grown in culture : 1) Repair of X-ray damage in surviving chinese hamster cells. Radiation Research 13, 556-593, (1960).

32) Gragg,R.L.,Humphrey,R.M. and Meyn,R.E. The response of chinese hamster ovary cells to fast-neutron radiotherapy beams. Radiation Research 71, pp.461-470, (1977).

33) Ngo,F.Q.H.,Utsumi,H.,Han,A. and Elkind,M.M. Sublethal damage repair : Is it independent of radiation quality? Lawrence Berkeley Laboratory; LBL-9931;Oct.1979.

34) Bianchi,M.Diehl,I.,Baarli,J. and Sullivan,A.H. Dose fractionation effects with negative pions. British Journal of Radiology,53,509-510,(1980).

35) Bianchi,M. and Diehl-Marshall,I. Effects of dose fractionation after irradiation with neutrons produced by 600 MeV protons. British Journal of Radiology,54,532-534,(1981).

36) Goldstein,L.S.,Phillips,T.L. and Ross,G.Y. Biological effects of accelerated heavy ions: II. Fractionated irradiations of intestinal crypt cells. Radiation Research 86,542-558,(1981).

37) Thomas,J.F.,Williamson,F.S.,Grain,D.A. and Ainsworth,E.A. Life shortening in mice exposed to fission neutrons and γ-rays. II. Duration-of-life and long-term fractionated exposures. Radiation Research 86, 573-579, (1981).

38) Hall,E.J. Radiobiology for the radiologist. Harper & Row, Publishers, Inc., 1973.

39) Skaarsgard,L.D. The biological properties of pions. Proceedings of the Sixth International Congress of Radiation Research, pp788-801,May 13-19 (1979),Tokyo.

40) Hall,E.J. and Lehnert,S. The biophysical properties of 3.9 GeV nitrogen ions. IV OER and RBE determinations using cultured mammalian cells. Radiation Research, Vol.55, pp.431-436, (1973).

41) Hall,E.J., Rossi,H.H., Kellerer,A.M., Goodman,L. and Marino,S. Radiobiological studies with monoenergetic neutrons. Radiation Research 54, 431-443 (1973).

42) Harrison,G.H. and Balcer-Kubiczek,E.K. The oxygen enhancement ratio for d(80)+(Be+Ta) and d(80)+(Ta+Be) neutrons. Radiation Research 83, 90-98 (1980).

43) Baarli,J.,Bianchi,M.,Hill,C.K.,Sullivan,A.H.,Tuyn,J.W.N. RBE and OER values of negative pion beams from growth inhibition of Vicia faba. Rad. and Environm. Biophysics 16,283-287 (1979).

44) Hall,E.J.,Brown,J.M.,Cavanagh,J. Radiosensitivity and the oxygen effect measured at different phases of the mitotic cycle using synchronously dividing cells of the root meristem of Vicia faba. Rad.Research,35, 622-634,(1968).

45) Weibezahn,K.F., Dertinger,H., Schlag,H., Luecke-Huhle,C. Biological effects of negative pions in monolayers and spheroids of chinese hamster cells. Rad. and Environm. Biophysics 16, pp.273-277, (1979).

46) Savage,J.R.K. Biology notes : Demonstrating cell division with Tradescantia. The School Science Review, 48, pp.771-782, (1967).

47) Conger,A.D. and Fairchild,L.M. A quick freeze method for making smear slides permanent. Stain Technology, 28, 281-283, (1963).

48) Weber,E. Grundriss der biologischen Statistik. Gustav Fischer Verlag Stuttgart 1972.

49) Bevington,P.R. Data reduction and error analysis for the physical sciences. McGraw-Hill Book Company 1969.

50) Johns,H.E. The physics of radiology. Charles C. Thomas. Publisher, Springfield Illinois, USA,1964.

51) Sullivan,A.H., Raffnsoe,C.R. Private communication (1978).

52) Fischer,Th., Fischer,U., Hagedorn,W., Hammel,G., Huerste,W., Kern,K., Kettle,R., Kleinschmidt,M., Lehmann,L., Moser,K., Roessle,E., Schmitt,H. SIN-Newsletter,No7, pp 14-17, October 1976.

53) Dunn,E. (compiled by) Quarterly report on the medium-energy physics program for the period ending october 31,1974. -Neutron spectrum and neutron scattering (Exp.56/125). LA-5845-PR; pp 51-53,(1975).

54) Marshak,R.E. Meson Physics. Mc.Graw-Hill Book Company,Inc. (1952).

55) Stephens,L.D. and Aceto,H. Neutron Dosim.,Vol.I,545,IAEA Vienna (1962).

56) Mc Caslin,J.B. Health Physics 2. 399, (1960).

57) Baarli,J.,Bakke,O.,Sullivan,A.H.,Tuyn,J.W.N. Dosimetry studies in a 600 MeV neutron beam. 3rd. Symp. on neutron dosimetry in biology and medicine, 1977 (Euratom,EUR5848,1978).

58) Baarli,J. and Sullivan,A.H. Dosimetry for radiobiological experiments with a 400 MeV neutron beam. Proc.Symp.Neutron Dosim. in Biol. and Med.; EURATOM, EUR4896, p.729, (1972).

59) Diehl,I. Messungen zur Energieabgabe von Protonen bei Bestrahlung von Gewebeaehnlichem Material mit Neutronen. Diplomarbeit, Institut fuer Experimentelle Kernphysik der Universitaet und des Kernforschungszentrums Karlsruhe, 1977.

60) Alsmiller,R.G., Armstrong,T.W., Coleman,W.A. The absorbed dose and dose equivalent from neutrons in the energy range 60 to

3000 MeV and protons in the energy range 400 to 3000 MeV. Nuclear Science and Engineering: 42, pp.367-381, (1970).

61) The Radiochemical Centre (Amersham) Californium-252 neutron sources. Technical bulletin 72/7.

62) Colvett,R.D.,Rossi,H.H.,Krishnaswany,V. Dose distributions around a 252-Californium needle. Phys. Med. Biol., Vol.17, No.3, pp.356-364, (1972).

63) Appel,H.,Bohmer,V.,Bueche,G.,Kluge,W.,Mathay,H. π^- beam studies using time of flight methods. Atomkernenergie, 27(3), p.177, (1976).

64) Nordell,B.,Baarli,J.,Sullivan,A.H. and Zielczynski,M. Determination of some parameters for pion radiobiology studies. Phys. Med. Biol., Vol.22, No.3, pp.466-475, (1977).

65) Baarli,J.,Bakke,O.,Bianchi,M.,Hill,C.and Sullivan,A.H. Radiobiology of negative pion beams of interest to cancer therapy. Invited paper presented at the Reunion d'Information sur la Radiotherapy par Neutrons,Orly,20-21 May,1977.

66) Dutrannois,J.,Hamm,R.N.,Turner,J.E.,Wright,H.H. Analysis of energy deposition in water around the site of capture of a negative pion by an oxygen or carbon nucleus. Phys. Med. Biol. Vol.17, pp.765-770, (1972).

67) Armstrong,T.W.,Chandler,K.C ORNL 4462, (1970).

68) Baarli,J.,Sullivan,A.H. Dosimetry problems of negative π^- mesons. Radiology Proc. of XIII Int. Congr. of Radiol.,Madrid, pp.426-431, Publ. Excerpta Medica, Amsterdam, 1973.

69) Klein,U. Messungen von Neutronenspektren nach der Absorption negativer Pionen in den biologisch relevanten Kernen ^{12}C, ^{14}N and ^{16}O. KfK-Ext.3/78-6,1978.

70) Mechtersheimer,G. Messung der Energiespektren von geladenen

Sekundaerteilchen nach der Absorption gestoppter negativer Pionen in Kohlenstoffkernen. KfK-Ext.3/78-7, 1978.

71) Muenchmeyer,D. Messung von Energiespektren und korrelierten geladenen Sekundaerteilchen nach der Absorption gestoppter negativer Pionen in sauerstoffhaltigen Targets. KfK-2786-B, Kernforschungszentrum Karlsruhe GmBH, Karlsruhe, 1979.

72) Randell,H. Messung der Energiespektren von geladenen Sekundaerteilchen, die nach der Absorption von gestoppten negativen Pionen in natuerlichem Calcium emittiert werden. KfK 2876 B, Kernforschungszentrum Karlsruhe GmBH, Karlsruhe, 1979.

73) Przybilla,G. Ein neues Monte-Carlo-Programm zur Berechnung der Energieuebertragung von einem π^--Mesonenstrahl auf ein gewebeaehnliches Phantom. KfK 3022, Kernforschungszentrum Karlsruhe GmBH, Karlsruhe,1980.

74) Mechtersheimer,G.,Bueche,G.,Klein,U.,Kluge,W.,Matthaey,H. and Muenchmeyer,D. Energy spectra of charged particles emitted following the absorption of stopped negative pions in ^{12}C nuclei. Nuclear Physics A324, 379-408,(1979).

75) Klein,U.,Bueche,G.,Kluge,W.,Matthaey,H.,Mechtersheimer,G. and Moline,A. Energy spectra of neutrons emitted following the absorption of stopped negative pions in light nuclei. Nuclear Physics A329, 339-353, (1979).

76) Bueche,G.and Przybilla,G. Distributions of absorbed dose from π^--meson beams calculated from a new Monte-Carlo program. Nuclear Instruments and Methods 179,321-341,(1981).

77) Midander,J., Revesz,L. The frequency of micronuclei as a measure of cell survival in irradiated cell populations. Int.J.Radiat.Biol. Vol 38,No2, pp.237-242,(1980).

78) Merz,T., Swanson,C.P., Cohn,N.S. Interaction of chromatid breaks produced by X-rays and radiomimetic compounds. Science, Vol.133, pp.703,705 (1961).

79) Miller,M.W., Colaiace,J.D. Radiation dose fractionation, mitotic index, and multiple fixation studies on chromosome aberrations in Vicia faba. Mutation Research, Vol10, pp449,462,(1970).

80) Savage,J.R.K. The use and abuse of chromosomal aberrations as an indicator of genetic damage. Intern.J.Environmental Studies, Vol1, pp233-240,(1971).

81) Savage,J.R.K. Private communication (1981).

82) Luecke-Huhle,C., Blakely,E.A., Chany,P.Y. and Tobias,C.A. Drastic G2 arrest in mammalian cells after irradiation with heavy-ion beams. Radiation Research 79,97-112 (1979).

83) Geard,C.R.,Polvas,S. and Marino,S. Monoenergetic neutron induced effects on cell progression in broad bean roots. Radiation Research 73, pp 160-167,1978.

84) Geard,C.R. and Marino S. Radiation induced delays in cell progression in Vicia faba root meristems. Radiation Research 69, pp 530-540,1977.

85) Neary,G.J.,Evans,H.J.,Tonkinson,S.M. and Williamson,F.S. The relative biological efficiency of single doses of fast neutrons and gamma rays on Vicia faba roots and the effect of oxygen. III. Mitotic delay. Int.J.Rad.Biol., Vol.3, p.230, 1959.

86) Raju,M.R.,Johnson,T.S.,Tokita,N.,Carpenter,S. and Jett,J.H. Differences in cell-cycle progression delays after exposure to ^{238}Pu α particles compared to X-rays. Radiation Research,84, pp 16-24,1980.

87) Diehl-Marshall,I., Bianchi,M. Induction of micronuclei after

irradiation with a 600 MeV neutron beam: Effects from 1 to 80 cGy. British Journal of Radiology, Vol.53, p.1104, (1980) (abstract).

88) Diehl-Marshall,I., Bianchi,M. Induction of micronuclei by irradiation with neutrons produced from 600 MeV protons. British Journal of Radiology, Vol.54, pp.530-532, (1981).

89) Dertinger,H., Luecke-Huhle,C., Schlag,H., Weibezahn,K.F. Negative pion irradiation of mammalian cells. II. Survival characteristics of monolayers and spheroids of Chinese hamster lung cells. Int. J. Radiat. Biol., Vol.29, No.3, pp.271-277, (1976).

90) Diehl-Marshall,I., Bianchi,M. Anzeichen einer linearen Dosis-Effekt Beziehung bei sehr kleinen Bestrahlungsdosen. Wissenschaftliche Tagung der "Schweizer Gesellschaft fur Strahlenbiologie und Strahlenphysik", Bern 7-8 November, p.107, (1980).

91) Diehl-Marshall,I., Bianchi,M. Linearity of micronuclei induction at low doses in bean roots. British Journal of Radiology, p.710, (abstract), (August 1981).

92) Diehl-Marshall,I., Bianchi,M. Micronuclei: A biological dosimeter for low doses. Presented at the Sixteenth Annual Meeting of the European Society for Radiation Biology. 7-10 September 1981, Jagiellonian University Krakow, Poland.

93) Underbrink,A.G., Woch,B. Evidence that the oxygen enhancement ratio for pink somatic\mutations in Tradescantia stamen hairs may approach unity at very low X-ray doses. Radiation Research, Vol.84, pp. 301-306, (1980).

94) Ritter,M.A., Cleaver,J.E. Tobias,C.A. High-LET radiations induce a large proportion of non-rejoining DNA breaks. Nature, Vol.266, No5603, pp.653-655,(1977).

95) Weibezahn,K.F.,Sexauer,C.,Coquerelle,T. Negative pion irradiation of mammalian cells. III. A comparative analysis of DNA strand breakage, repair and cell survival after exposure to π^--mesons and X-rays. Int. J. Radiat. Biol., Vol.38, No.4, pp.365-371, (1980).

96) Grote,S.J., Joshi,G.P., Revell,S.H., Shaw,C.A. A method for the scrutiny of life mammalian cells in culture and for the measurement of the proliferative ability after X-irradiation. Int. J. Radiat. Biol., Vol.39, No.4, pp.377-394, (1981).

97) Grote,S.J., Joshi,G.P., Revell,S.H., Shaw,C.A. Observations of radiation-induced chromosome fragment loss in life mammalian cells in culture, and its effect on colony forming ability. Int. J. Radiat. Biol., Vol.39, No.4, pp.395-408, (1981).

98) Holt,P.D. The range of electrons below 1KeV. Charged Particle Tracks in Solids and Liquids. Proceedings of the second L.H.Gray Conference April(1969). Published by the Institute of Physics and the Physical Society. London, Conference Series No8.

99) Sparrow,A.H.,Underbrink,A.G. and Rossi,H.H. Mutations induced in Tradescantia by small doses of X-rays and neutrons: Analysis of dose-response curves. Science,176, pp 916-918,1972.

100) Furcinitti,P.S., Todd,P. Gamma rays: Further evidence for a lack of threshold dose for lethality to human cells. Science,Vol.206, pp. 475,477 ,26.Oct.1979.

101) Lloyd,D.C., Purrot,R.J., Doplphin,G.W., Dawn Bolton, Edwards,A.A., Corp,M.J. The relationship between chromosome aberrations and low LET radiation dose to human lym-

phocytes. Int. J. Radiat. Biol., Vol.25, No.1, pp.75-90, (1975).

102) Goldstein,L.S., Phillips,T.L., Ross,G.Y. Enhancement by fractionation of biological peak-to-plateau relative biological effectiveness ratios for heavy ions. Int. J. Radiation Oncology Biol. Phys., Vol.4, pp.1033-1037.

103) Wulf,H., Miltenberger,H.G., Dertinger,H., Kraft,G. Heavy ion irradiation of mammalian tissue culture cells. Sixteenth Annual Meeting of the European Society for Radiation Biology. 7-10 September 1981, Jagiellonian University Krakow, Poland.

104) Vogel,H.H., Dickson,H. Dose and dose rate effects of fission neutrons and ^{60}Cobalt gamma rays on mammary tumor induction. Sixteenth Annual Meeting of the European Society for Radiation Biology. 7-10 September 1981, Jagiellonian University Krakow, Poland.

105) Bateman,J.L., Rossi,H.H., Kellerer,A.M., Robinson,C.V., Bond,V.P. Dose dependence of fast neutron RBE for lens opacification in mice. Radiat. Res., Vol.51, pp.381-390, (1972).

106) Vogel,H.H. Mammary gland neoplasms after fission neutron irradiation. Nature (London) Vol.222, pp.1279-1281, (1969).

107) Biola,M.T., LeGo,R., Ducatez,G., Dacher,J., Bourguignon,M. Formation de chromosome dicentriques dans les lymphocytes humains soumis in vitro a un flux de rayonnement mixte (gammas, neutrons). In Advances in Physical and Biological Radiation Detectors, pp.633-645. International Atomic Energy Agency, Vienna, 1971.

108) Hall,E.J., Rossi,H.H., Kellerer,A.M., Goodman,L., Marino,S. Radiobiological studies with monoenergetic neutrons. Radi-

ation Research, Vol.54, pp.431-443, (1973).

109) Field,St.B. The relative biological effectiveness of fast neutrons for mammalian tissues. Radiology, Vol.93, pp.915-920, (1969).

110) Di Paola,M.,Coppola,M.,Baarli,J.,Bianchi,M.,Sullivan,A.H. Biological responses to various neutron energies from 1 to 600 MeV. II. Lens opacification in mice. Radiation Research Vol.84, pp.453-461,(1980).

111) Raju,M.R., Richman,C. GANN Monograph 9 (Maruzen Co.Ltd.,Tokyo) p.105, (1970).

112) Raju,M.R., Gnanapurani,M., Stackler,B., Martins,B.I., Madhvanath,U., Howard,J., Lyman,J.T., Mortimer,R.K. Radiation Research, Vol.47, p.635, (1971).

113) Richman,S.P., Richman,C., Raju,M.R., Schwartz,B. Radiation Research Suppl., Vol.7, p.182, (1967).

114) Loughman,W.D., Feola,J.M., Raju,M.R., Winchell,H.S. Radiation Research, Vol.34, p.56, (1968).

115) Raju,M.R., Gnanapurani,M., Martins,B.I., Richman,C., Barendsen,G.W. Brit. J. Radiol., Vol.45, p.178, (1972).

116) Baarli,J., Bianchi,M., Sullivan,A.H., Quintaliani,M. Intern. J., Radiat. Biol., Vol 19, p.537, (1971).

117) Vulpis,N. et.al. Unpublished data, (1981).

118) Molls,M. Streffer,C., Zamboglou,N. Micronucleus formation in preimplanted mouse embryos cultured in vitro after irradiation with X-rays and neutrons. Int. J. Radiat. Biol., Vol.39, No.3, pp.307-314, (1981).